

Induction of autophagy by spermidine promotes longevity

Tobias Eisenberg¹, Heide Knauer¹, Alexandra Schauer¹, Sabrina Büttner¹, Christoph Ruckenstuhl¹, Didac Carmona-Gutierrez¹, Julia Ring¹, Sabrina Schroeder¹, Christoph Magnes², Lucia Antonacci¹, Heike Fussi¹, Luiza Deszcz^{3,4}, Regina Hartl^{3,4}, Elisabeth Schraml⁵, Alfredo Criollo^{6,7,8}, Evgenia Megalou⁹, Daniela Weiskopf¹⁰, Peter Laun¹¹, Gino Heeren¹¹, Michael Breitenbach¹¹, Beatrix Grubeck-Loebenstain¹⁰, Eva Herker¹², Birthe Fahrenkrog¹³, Kai-Uwe Fröhlich¹, Frank Sinner², Nektarios Tavernarakis⁹, Nadege Minois^{3,4,14}, Guido Kroemer^{6,7,8,15} and Frank Madeo^{1,15}

Ageing results from complex genetically and epigenetically programmed processes that are elicited in part by noxious or stressful events that cause programmed cell death. Here, we report that administration of spermidine, a natural polyamine whose intracellular concentration declines during human ageing, markedly extended the lifespan of yeast, flies and worms, and human immune cells. In addition, spermidine administration potently inhibited oxidative stress in ageing mice. In ageing yeast, spermidine treatment triggered epigenetic deacetylation of histone H3 through inhibition of histone acetyltransferases (HAT), suppressing oxidative stress and necrosis. Conversely, depletion of endogenous polyamines led to hyperacetylation, generation of reactive oxygen species, early necrotic death and decreased lifespan. The altered acetylation status of the chromatin led to significant upregulation of various autophagy-related transcripts, triggering autophagy in yeast, flies, worms and human cells. Finally, we found that enhanced autophagy is crucial for polyamine-induced suppression of necrosis and enhanced longevity.

As an organism ages, the fate of individual cells is dictated by apoptotic or necrotic cell death pathways, as well as autophagy, as a cytoprotective process^{1–3}. Until recently, necrosis has been regarded as a form of accidental, unregulated cell death resulting from severe chemical or physical disruption of the plasma membrane, which contrasts with the subtly regulated, ‘programmed’ apoptotic death. Recent research suggests, however, that the occurrence and course of necrosis can be subject to complex controlled processes and that necrosis can therefore also be ‘programmed’^{4,5}.

During replicative ageing of yeast, activation of the phylogenetically conserved ageing regulator Sir2, an NAD⁺-dependent histone deacetylase, has been found to promote longevity⁶ and to be important (among other sirtuins) for lifespan extension under various conditions^{7,8}. Epigenetic hypoacetylation of histones has since been regarded as a key process during healthy ageing^{6,9–12}. Chronological ageing of yeast cells follows molecular pathways that are shared with those dictating longevity of non-dividing post-diauxic cells of higher eukaryotes^{2,13}. One of these pathways is regulated by Tor kinases, and decreased TORC1 activity can promote longevity of various organisms^{14–16}. TORC1 activity

is known to negatively regulate autophagy, the major lysosomal degradation pathway that recycles damaged and potentially harmful cellular material. Accordingly, autophagy counteracts cell death and prolongs lifespan in various models of ageing^{17,18}.

Among the multiple biochemical correlates of ageing, a decrease in intracellular polyamines has been described in ageing mammalian cell culture and during human ageing in various organs including serum¹⁹. However, it has remained unclear whether depletion of polyamines is a cause or a consequence of the ageing process. Here, we show that administration of exogenous spermidine, a naturally occurring polyamine, extends lifespan in various models of ageing through epigenetic modifications, induction of autophagy and suppression of necrosis.

RESULTS

Spermidine application suppresses ageing in yeast, flies, worms, human cells and mice.

A decrease in polyamines has been repeatedly correlated with the ageing process, although its potential causality has not yet been investigated.

¹Institute of Molecular Biosciences, University of Graz, 8010 Graz, Austria. ²Institute of Medical Technologies and Health Management, Joanneum Research, Graz, Austria. ³Research Institute of Molecular Pathology (IMP), Vienna, Austria. ⁴Institute of Molecular Biotechnology (IMBA), Austrian Academy of Sciences, Vienna, Austria. ⁵Institute of Applied Microbiology, University of Natural Resources and Applied Life Sciences, Vienna, Austria. ⁶INSERM, U848; 94805 Villejuif, France. ⁷Institut Gustave Roussy, 94805 Villejuif, France. ⁸University Paris Sud, Paris-11, 94805 Villejuif, France. ⁹Institute of Molecular Biology and Biotechnology, Foundation for Research and Technology-Hellas, 70013, Heraklion, Crete, Greece. ¹⁰Institute for Biomedical Ageing Research, Austrian Academy of Sciences, 6020 Innsbruck, Austria. ¹¹Department of Cell Biology, Division of Genetics, University of Salzburg, 5020 Salzburg, Austria. ¹²Gladstone Institute of Virology and Immunology, San Francisco, CA 94158, USA. ¹³M.E. Mueller Institute for Structural Biology, Biozentrum, University of Basel, 4056 Basel, Switzerland. ¹⁴Current address: School of Biology, University of St Andrews, St Andrews, Scotland, Fife KY16 9AJ, UK.

¹⁵Correspondence should be addressed to F.M. or G.K. (e-mail: frank.madeo@uni-graz.at; kroemer@orange.fr)

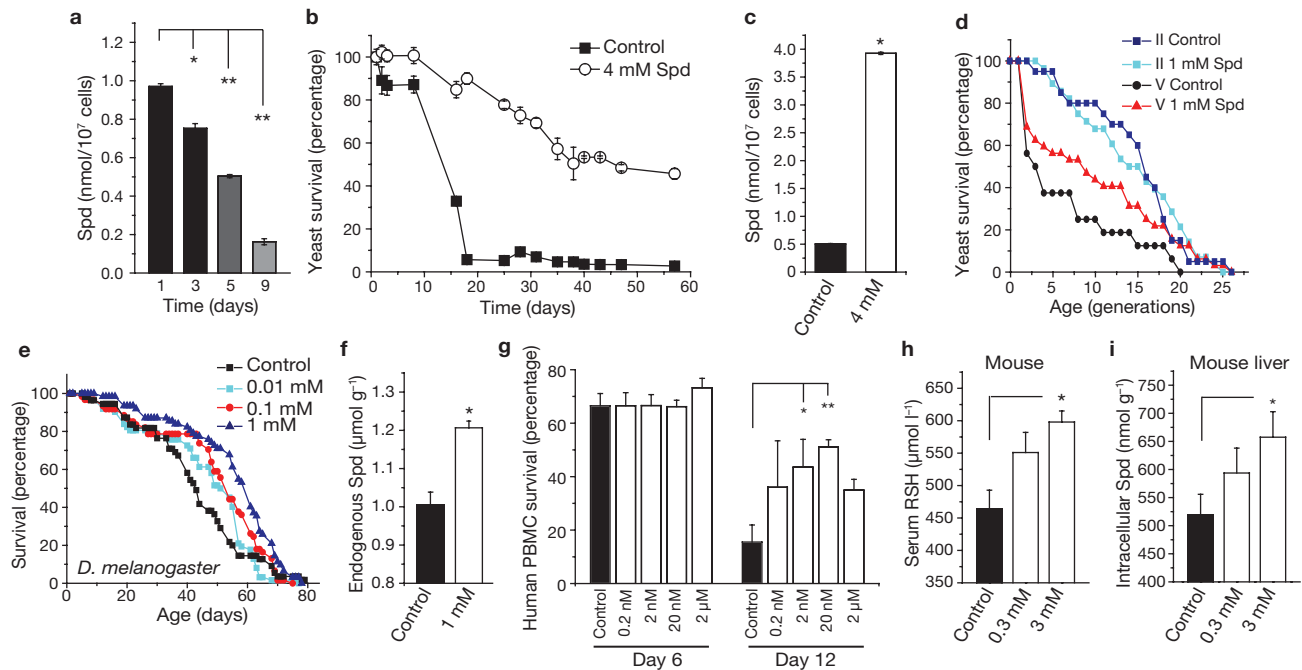


Figure 1 Application of spermidine extends the lifespan of yeast, flies and human immune cells, and inhibits oxidative stress in ageing mice. **(a)** Intracellular levels of spermidine (Spd) in chronologically ageing wild-type yeast. Data represent means \pm s.e.m. ($n = 3$; * $P < 0.05$ and ** $P < 0.001$). **(b)** Survival determined by clonogenicity during chronological ageing of wild-type yeast (BY4741) cells with (o) and without (■) addition of spermidine (4 mM) at day 1. Data represent means \pm s.e.m. ($n = 5$). **(c)** Intracellular levels of spermidine in chronologically ageing wild-type yeast cells cultured with (open bar) or without (closed bar) spermidine (4 mM) for 5 days. Data represent means \pm s.e.m. ($n = 3$; ** $P < 0.001$). **(d)** Replicative lifespan analysis of BY4741 wild-type yeast cells after separation into old (fraction V) and young (fraction II) cells by elutriation centrifugation. The remaining lifespan with or without (control) spermidine (1 mM, applied after elutriation) on 2% glucose synthetic complete medium is shown. **(e)** Survival determined by the age-specific number of dead individuals of female *Drosophila* with

and without (control) supplementation of food with various concentrations of spermidine (as indicated). A representative ageing experiment of at least 50 flies per sample is shown. **(f)** Endogenous spermidine of female *Drosophila* fed for 48 h with food supplemented by 1 mM spermidine, compared with normal food (control). Data represent means \pm s.e.m. ($n = 3$; * $P < 0.01$). **(g)** Survival determined by annexin V/7-AAD co-staining (unstained cells were considered as viable) of human immune cells (PBMC) cultured for 6 and 12 days in the absence (black bar) or presence (white bars) of various spermidine concentrations (as indicated). Data represent means \pm s.e.m. of 3 independent experiments (each performed on PBMC from different donors). * $P < 0.05$ and ** $P < 0.01$. **(h, i)** Free thiol group (RSH) concentration in serum **(h)** and intracellular spermidine concentration in hepatocytes **(i)** of ageing mice with (open bars) or without (closed bar) supplementation of drinking water with spermidine (0.3 and 3 mM) for 200 days. Data represent mean \pm s.e.m. ($n = 3$; * $P < 0.05$ and ** $P < 0.01$).

To address this, we applied spermidine to chronologically ageing yeast cells, which (as we show here) show a decline in the levels of endogenous polyamines (Fig. 1a) and a progressive loss in clonogenic survival^{1,2,20}. Exogenous supply of spermidine to ageing wild-type BY4741 cells (at day 1) caused a marked increase in lifespan by a factor of up to four times that of untreated cells, as determined in clonogenic assays that monitored the frequency of viable cells (Fig. 1b). Similar results were obtained using wild-type DBY746 cells (Supplementary Information, Fig. S1a). Spermidine supplementation also led to a stable increase in intracellular spermidine levels in ageing cells (Fig. 1c), which would otherwise show a decrease in endogenous spermidine levels (Fig. 1a).

Whereas chronological ageing is a model for ageing of post-mitotic tissues, replicative ageing of yeast models the lifespan of dividing cells in higher eukaryotes. Both ageing systems are interrelated, as replicatively old cells die early during chronological ageing²¹. We therefore analysed the differential effect of spermidine on replicatively young and old cells obtained by elutriation²². The remaining replicative lifespan of old cells was significantly increased by spermidine (Fig. 1d, fraction V cells, $P < 0.02$), whereas no apparent effect was seen on the remaining lifespan of replicatively young cells (fraction II cells, Fig. 1d). Thus, spermidine retards chronological ageing and also

rejuvenates replicatively old cells. Improved longevity often correlates with increased stress resistance²³. Accordingly, long-lived spermidine-treated cells showed a strong resistance to stress inflicted by heat shock or H_2O_2 treatment (Supplementary Information, Fig. S1b).

In an attempt to extend the lifespan of a complete metazoan organism, we supplemented ordinary food of the fruitfly *Drosophila melanogaster* with spermidine. Optimal doses of spermidine increased the mean lifespan of flies up to 30% (Fig. 1e, $P = 0.0002$ for 1 mM; for mean lifespans and replicates see Supplementary Information, Fig. S2). Measurement of endogenous polyamines confirmed that spermidine supplementation stably increased intracellular spermidine levels by about 20%, compared with controls (Fig. 1f). Notably, putrescine (a polyamine interconvertible with spermidine) was undetectable in control samples but clearly present in spermidine-fed flies (~ 100 nmol g^{-1}), indicating that spermidine was indeed taken up and metabolized by the flies (data not shown). Similarly, we found that polyamines prolonged the mean and the maximum lifespan of the nematode *Caenorhabditis elegans*. Supplementation of regular food with spermidine (0.2 mM) extended the nematode lifespan by up to 15% (Fig. 7i, $P < 0.0001$).

We next investigated whether polyamines also enhanced the lifespan of human peripheral blood mononuclear cells (PBMC), and monitored

survival using annexin V/7-AAD co-staining (unstained cells were regarded as viable). After 12 days, only 15% of cells in the control PBMC cultures survived, whereas up to 50% of the cells survived after addition of spermidine (20 nM; Fig. 1g). Unexpectedly, the rescuing effect did not involve any inhibition of apoptosis, as the percentage of apoptotic cells (annexin V⁺/7-AAD⁻) was not influenced by spermidine. Instead, cell death associated with membrane rupture, which is indicative of necrosis (annexin V⁺/7-AAD⁺ cells), was markedly reduced (Supplementary Information, Fig. S3a).

One of the most widely accepted theories of ageing is the free radical theory, which attributes ageing to accumulating oxidative stress²⁴. In rodents, the level of oxidative stress and protein damage increases consistently with age, as observed by a decline in free thiol groups in serum proteins²⁵. Feeding mice with spermidine (3 mM, added to the drinking water) for 200 days increased the serum level of free thiol groups by about 30%, indicating reduced age-related oxidative stress (Fig. 1h). Notably, such an increase in free thiol groups is comparable to the natural decline that has been observed during the course of ageing (between young and old rodents)²⁵. Again, intracellular spermidine levels were significantly increased by exogenous spermidine supplementation, as determined in liver cells (Fig. 1i). Together, these data indicate that exogenous supplementation of spermidine can retard cellular and organismal ageing in several species.

Polyamine depletion decreases yeast lifespan and increases necrosis

We next investigated the effect of polyamine depletion on yeast chronological ageing, using a yeast strain that is deficient in *SPE1* (Δ *spe1*) and hence unable to synthesize polyamines. Polyamine depletion, as confirmed by measurement of intracellular spermidine (Fig. 2a), markedly shortened lifespan, which could subsequently be restored by supplementation with 0.1 mM spermidine or its precursor putrescine (Fig. 2b, data not shown). Note that in this case, a low spermidine concentration was chosen for complementation, which did not enhance wild-type survival *per se* (Fig. 2b).

Consistent with the free radical theory of ageing²⁴, we observed an enhanced accumulation of oxygen radicals after disruption of *SPE1*, as indicated by the increased superoxide-mediated conversion of cell-permeable non-fluorescent dihydroethidium (DHE) to fluorescent ethidium (Eth), which remains trapped in the cells (Fig. 2c, d). Close inspection of phenotypical cell death markers revealed that the enhanced death rate of Δ *spe1* cells was associated with a rapid loss of membrane integrity, although apoptotic markers remained constant (Fig. 2e; see Supplementary Information, Results and Discussion for more details). We conclude therefore that depletion of intracellular polyamines can precipitate premature chronological ageing through non-apoptotic, presumably necrotic death of yeast cells.

Spermidine prolongs lifespan in various ageing models in a pH-independent fashion

Very few studies have addressed the mechanisms of necrotic cell death in a systematic fashion. In *C. elegans*, acidification of the cytosol is reportedly required for necrotic cell death, whereas alkalization has a cytoprotective effect^{26,27}. Furthermore, recent reports indicate that one of the major causes of yeast chronological ageing is the excessive production of acetic acid²⁸. Consistent with this view, administration of spermidine to

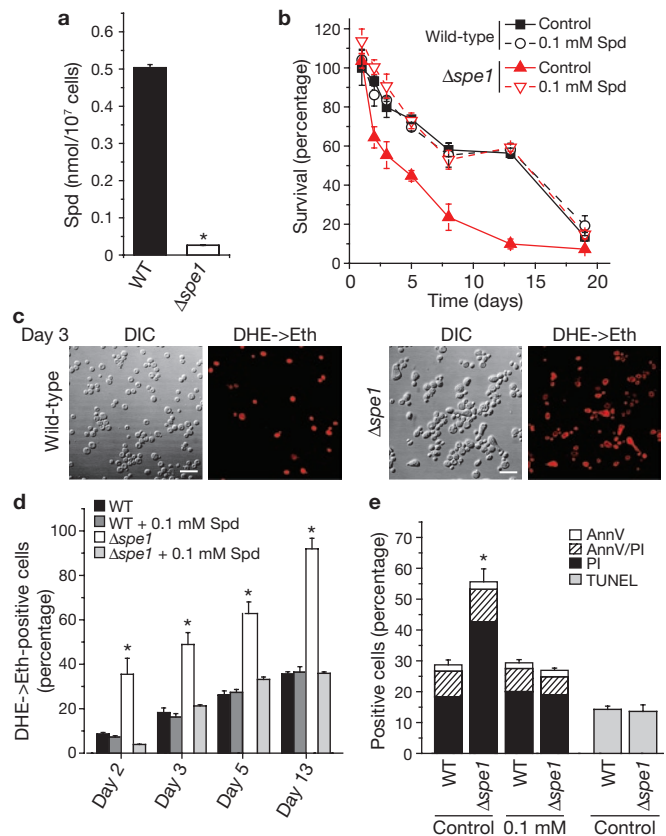


Figure 2 Polyamine depletion shortens yeast chronological lifespan evoking markers of oxidative stress and necrosis. (a) Intracellular spermidine of five-day-old Δ *spe1* cells, compared with wild-type cells. Data represent means \pm s.e.m. ($n = 3$; $*P < 0.001$). (b) Chronological ageing of wild-type (\blacksquare , \circ) and polyamine-depleted Δ *spe1* (\blacktriangle , ∇) yeast cells with (open symbols) and without (closed symbols) supplementation of low doses of spermidine. Data represent means \pm s.e.m. ($n = 4$). Cells were tested for cell death markers at day 3. (c) Fluorescence microscopy of DHE-to-Eth conversion in wild-type and Δ *spe1* cells indicating ROS production. Scale bars, 10 μ m. (d) Quantification (FACS analysis) of ROS accumulation using DHE-to-Eth conversion of wild-type (WT) and Δ *spe1* cells with and without supplementation of low doses of spermidine. Data represent means \pm s.e.m. ($n = 4$; $*P < 0.001$). (e) Quantification (FACS analysis) of phosphatidylserine externalization and loss of membrane integrity using annexin V/PI co-staining (at day 5) and of DNA fragmentation using TUNEL staining (at day 3) of chronologically ageing wild-type (WT) and Δ *spe1* cells with or without supplementation of 0.1 mM spermidine as indicated. Data represent means \pm s.e.m. ($n = 3$; $*P < 0.001$).

chronologically ageing yeast, or alkalization of the medium with NaOH, prolonged yeast lifespan and increased the extracellular and cytosolic pH (data not shown) but in a manner strictly dependent on intracellular polyamines (Supplementary Information, Fig. S3b; see Supplementary Results and Discussion for further details).

Chronological ageing of yeast in water, which is independent of the pH because of repeated removal of produced acid²⁸, reportedly relies on phylogenetically conserved molecular mechanisms²⁹ similar to ageing under standard conditions³⁰. We therefore transferred stationary yeast cells preloaded with high concentrations of spermidine (8 mM) to water at an early stage during ageing, while adjusting the pH of spermidine cultures to that of spermidine-free controls. Under these conditions, spermidine continued to extend the chronological

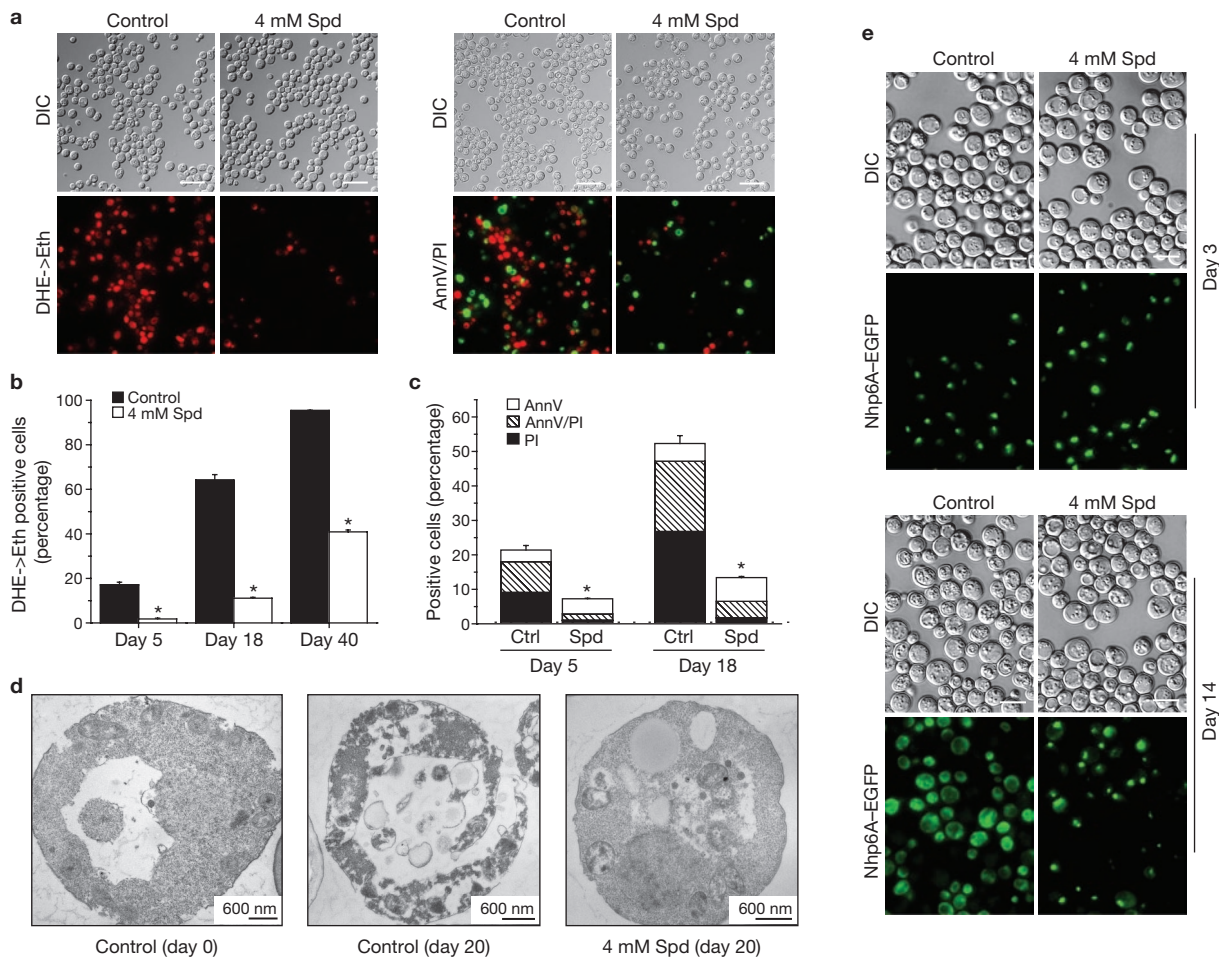


Figure 3 Spermidine application suppresses necrotic cell death. (a) Fluorescence microscopy of DHE→Eth conversion and annexin V (green)/PI (red) co-staining of wild-type cells at day 18 of the chronological ageing experiment shown in Fig. 1b. Scale bars, 10 μ m. (b, c) Quantification of DHE→Eth conversion (b) and annexin V/PI co-staining (c) using FACS analysis performed at indicated time-points of the chronological ageing experiment shown in Fig. 1b. Data represent means \pm s.e.m.

($n = 3$; * $P < 0.001$). (d) Electron microscopy of young log-phase cells (day 0) and of 20-day-old wild-type cells aged without (control) or with spermidine (4 mM). Representative cells are shown (for an overview see Supplementary Information, Fig. S3c). (e) Fluorescence microscopy of chronologically aged wild-type cells (day 3 and 14) expressing an EGFP-tagged version of the yeast HMGB1 homologue (Nhp6A-EGFP) with or without (control) addition of 4 mM spermidine. Scale bars, 5 μ m.

lifespan and reduce ROS levels (Fig. 6e, f). In summary, spermidine is able to extend lifespan and to inhibit age-related oxidative stress in a pH-independent fashion.

Spermidine application counteracts age-induced necrotic cell death

Determination of cell death markers revealed that markers of necrosis (loss of membrane integrity) and oxidative stress (DHE→Eth conversion) were markedly diminished with spermidine treatment (Fig. 3a–c; see Supplementary Discussion for details). Consistently, electron microscopy of old cells (day 20) showed necrotic disintegration of subcellular structures and rupture of the plasma membrane, whereas the ultrastructure of spermidine-treated samples of the same age resembled that of young cells (Fig. 3d). Nuclear release of the high mobility group Box 1 protein (HMGB1), a chromatin bound non-histone protein, is a defining feature of necrosis in mammalian cells³¹. Fluorescence microscopy detected the nucleo–cytosolic translocation of the yeast HMGB1 homologue Nhp6Ap (rendered visible with an EGFP tag) after 14 days of ageing (Fig. 3e). Again, this necrotic feature was prevented by application

of spermidine (Fig. 3e). Thus, spermidine treatment protects against ageing through the inhibition of necrosis.

Hypoacetylation of histone H3 correlates with spermidine-induced longevity

As the budding index and mutation frequency during ageing³² remained largely unaffected by application of spermidine (Supplementary Information, Fig. S3d, e and Results and Discussion), we considered the possibility that epigenetic modifications, rather than regrowth of death-resistant mutants¹, might regulate lifespan extension. Histone deacetylation, a key event in epigenetic chromatin modification⁹, is associated with healthy ageing in many organisms¹¹ and deacetylation of specific lysyl residues was suggested to be crucial for yeast lifespan extension, at least during replicative ageing^{6,12}. We therefore analysed the effects of spermidine on the level of histone acetylation by using antibodies that specifically detect acetylated lysyl residues located at the amino-terminal tail of histone H3 (Lys 9, 14 and 18). The improved lifespan of ageing wild-type cells treated with spermidine correlated with hypoacetylation of histone H3 at all acetylation sites

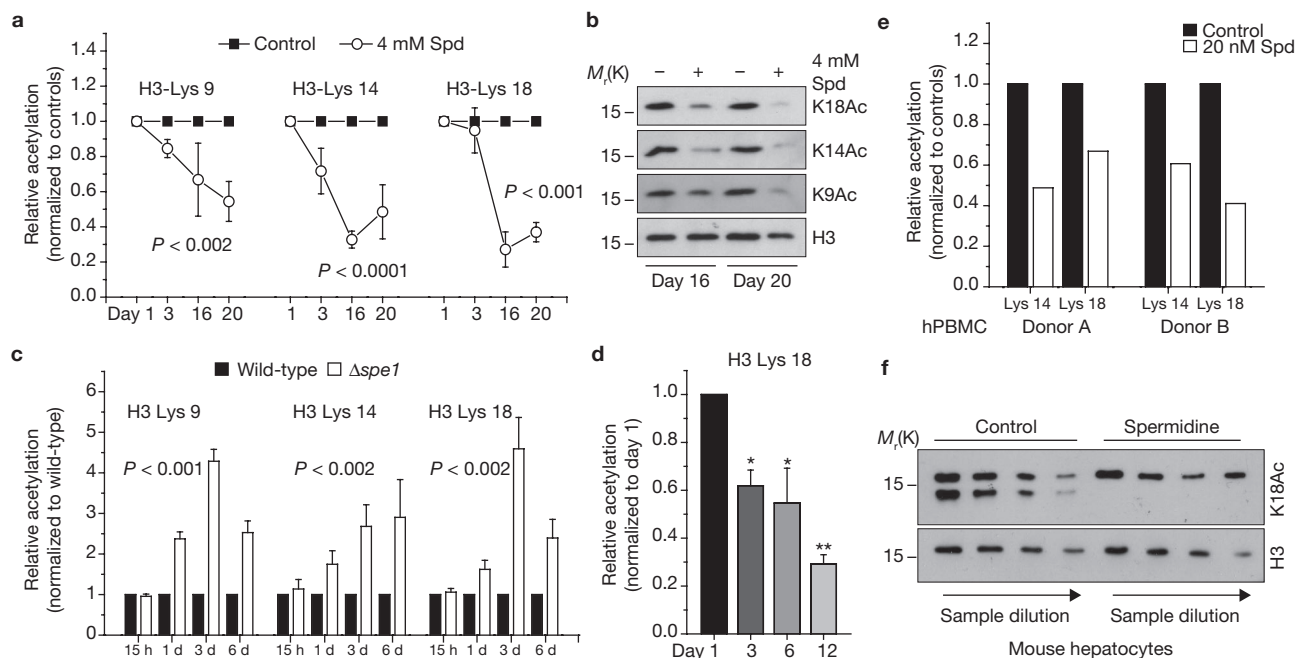


Figure 4 Lifespan extension by spermidine application is accompanied by epigenetic hypoacetylation of histone H3. **(a)** Relative acetylation (normalized to controls at each day) of indicated histone H3 Lys residues determined by quantification of immunoblot analysis. A representative blot using site specific antibodies is shown in **b**. Data represent means \pm s.e.m. ($n = 3$). Serial dilutions of protein extracts were applied in western blots to verify linearity before quantification (examples are shown in Supplementary Information, Fig. S4). For calculation details see section on Methods. P values indicate the result of a two-factor ANOVA corrected by Bonferroni post hoc test. **(b)** Immunoblot of whole-cell extracts of wild-type cells chronologically aged to designated time-points with (+) or without (-) spermidine application. Blots were probed with antibodies against total histone H3 or H3 acetylation sites at the indicated Lys residues. Full scans of blots are available in Supplementary Information, Fig. S5. **(c)** Relative acetylation (normalized to wild-type controls at each day) of indicated

histone H3 Lys residues of $\Delta spe1$ cells (open bars), compared with wild-type cells (closed bars) during chronological ageing. Data represent means \pm s.e.m. ($n = 3$). P values indicate the result of a two-factor ANOVA corrected by Bonferroni post hoc test. **(d)** Relative acetylation (normalized to day 1) of histone H3 Lys 18 residue of chronologically ageing wild-type cells. Data represent means \pm s.e.m. ($n = 3$). **(e)** Relative acetylation (normalized to controls) of histone H3 Lys 14 and 18 residues of cultured human PBMC after 6 days of incubation with or without 20 nM spermidine. Data represent quantification of two independent experiments performed with cells obtained from two different donors. **(f)** Immunoblot analysis of liver cell extracts (applied in serial dilutions) obtained from mice fed with 3 mM spermidine for 200 days and respective control mice of the same age. Blots were probed with antibodies recognizing total histone H3 (C-terminal epitope) or specific for acetylated lysine 18 residue (N-terminal epitope). Full scans of blots are available in Supplementary Information, Fig. S5.

monitored (Fig. 4a, b; see Methods and Supplementary Information, Fig. S4 for details of quantification). Conversely, premature death of ageing *SPE1*-deleted cells was accompanied by hyperacetylation of histone H3 (Fig. 4c; Supplementary Information, Fig. S4c). These results suggest that global deacetylation and polyamines are both connected to the extension of chronological lifespan in yeast, yet cannot serve as a final proof of causality between histone deacetylation and longevity. Interestingly, the level of histone acetylation decreased during ageing of wild-type cells kept under standard culture conditions (Fig. 4d), perhaps as an adaptive anti-ageing mechanism. Accordingly, acceleration of this adaptive response (histone hypoacetylation) by administration of exogenous spermidine led to longevity.

Next, we investigated whether spermidine would affect histone H3 acetylation during ageing in mammalian cells. Exogenous supply of spermidine (20 nM) to human PBMC greatly reduced the acetylation levels of Lys 14 and 18 after as few as 6 days of incubation (Fig. 4e; Supplementary Information, Fig. S4d).

Hepatocytes from mice fed with spermidine for 200 days showed similar levels of histone H3 acetylation at Lys 14 or 18, compared with liver cells from control mice (Fig. 4f). However, an electrophoretically more mobile form of histone H3 appeared in extracts from control mice,

suggesting its proteolytic processing³³. Note that we detected the processed form of histone H3 only when using acetylated Lys-specific antibodies that recognize H3 at an N-terminal epitope and not when using the antibody against total histone H3 that recognizes a carboxy-terminal epitope. These observations indicate a C-terminal cleavage of the histone, however, at a different site compared with recent findings in mouse embryonic stem cells³³. This physiological age-related processing of histone H3 was completely inhibited by feeding mice spermidine (Fig. 4f). Our findings suggest that spermidine-inducible modification of histone H3, as with yeast lifespan regulation, also coincides with organismal ageing, although in a more complex fashion.

Spermidine inhibits HAT activity, which causes longevity and suppression of necrosis

As the role of the Sir2p deacetylase is well established in replicative ageing^{7,11,12}, we tested its potential involvement (and that of 27 other proteins implicated in histone acetylation) in polyamine-promoted longevity during chronological ageing. Deletion of *SIR2* or any other sirtuin did not abrogate the ability of spermidine to extend chronological lifespan (Supplementary Information, Table S1 and data not shown). Instead, the pro-survival effect of spermidine was partially abrogated in two

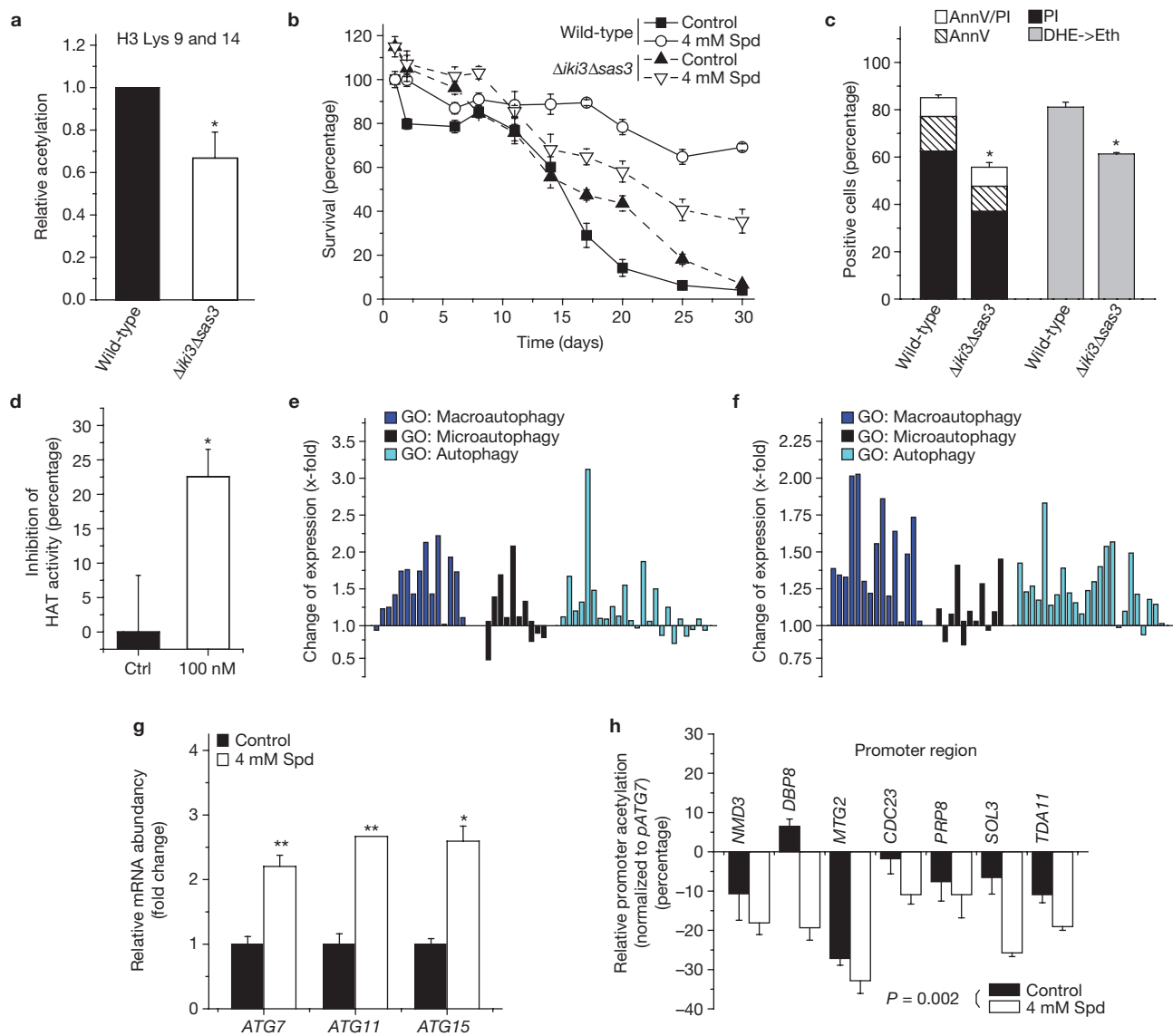


Figure 5 Spermidine-induced longevity is mediated by inhibition of HAT activity and correlates with upregulation of autophagy-related genes. (a) Relative acetylation of histone H3 Lys 9 and 14 residues determined by quantification of immunoblot analysis performed at day 20 of the ageing experiment shown in panel b. Data represent means \pm s.e.m. ($n = 3$; $*P < 0.05$). (b) Chronological ageing of wild-type (\blacktriangle , \circ) and $\Delta iki3\Delta sas3$ (\blacktriangle , ∇) with (open symbols) or without (closed symbols) addition of spermidine (4 mM) at day 1. Data represent means \pm s.e.m. ($n = 4$). (c) Quantification (FACS analysis) of phosphatidylserine externalization and loss of membrane integrity (annexinV/PI containing) as well as ROS production (DHE \rightarrow Eth conversion) performed at day 20 of the experiment shown in b. Data represent means \pm s.e.m. ($n = 4$; $*P < 0.001$). (d) Relative inhibition of histone acetyltransferase activity (HAT-activity) by spermidine determined by an *in vitro* HAT-activity assay of yeast nuclear extracts of wild-type cells. Data represent means \pm s.e.m. of three independent experiments ($*P = 0.024$). (e, f) Transcriptional change (obtained by Affymetrix array) by spermidine treatment of all autophagy-related genes categorized into

GO terms of macroautophagy (GO:0016236), microautophagy (GO:0016237) or autophagy in general (GO:0006914) at day 3 (e) and day 10 (f) of chronological ageing yeast. Data represent means of two independent arrays from independent biological samples. (g) Relative change of *ATG7*, *ATG11* and *ATG15* mRNA levels by spermidine supplementation (normalised to controls) after ten days of chronological ageing as determined by reverse transcriptase real-time PCR. Data represent means \pm s.e.m. ($n = 3$; $*P < 0.05$ and $**P < 0.01$). (h) Relative histone H3 Lys 18 acetylation of indicated promoter regions normalized to the acetylation of *ATG7* promoter (*pATG7*) determined by chromatin immunoprecipitation with H3-K18Ac specific antibody and subsequent quantification of precipitated promoter DNA using quantitative real time PCR. Signals specific for indicated promoter regions were initially compared with non-immunoprecipitated samples and afterwards normalized to the *pATG7* signals. Data represent means \pm s.e.m. ($n = 3$). The P value was calculated using a two-factor ANOVA with promoter and condition (treated and non-treated) as independent factors.

of the screened knockout strains, $\Delta iki3$ and $\Delta sas3$ (see Supplementary Information, Table S1, Results and Discussion for details). Deletion of *IKI3*, an essential subunit of the histone acetylating elongator complex, is known to reduce histone H3 acetylation at Lys 14 (ref. 34). Similarly, the HAT Sas3p is known to preferentially acetylate histone H3 at Lys 14

(ref. 35), which is one of the sites where acetylation depends on the abundance of endogenous or administrated spermidine (see above). Driven by this coincidence, we generated the double mutant $\Delta iki3\Delta sas3$, and investigated the extent to which this double mutant would phenocopy the effects of spermidine treatment. *IKI3* and *SAS3* double-mutant cells

showed reduced histone H3 acetylation (Fig. 5a), as well as improved survival during chronological ageing when compared with wild-type controls (Fig. 5b, $P < 0.002$). In addition, the double disruptants produced less ROS and fewer of these cells underwent necrotic cell death, compared with control cells (Fig. 5c). This finding is consistent with the interpretation that activity of the two acetyltransferases would be (co-) responsible for age-induced cell death.

Combined knockout of *IKI3* and *SAS3* did increase the lifespan of yeast cells, but failed to mimic in quantitative terms the lifespan-prolonging effect of spermidine, perhaps because epigenetic ageing processes are regulated by more than two enzymes. An *in vitro* assay revealed that spermidine efficiently inhibited general HAT activity in extracts of isolated yeast and mammalian nuclei (Fig. 5d and data not shown). These results suggest that spermidine-mediated anti-ageing effects are achieved through direct inhibition of HAT activity, although multiple other interactions between polyamines and histone acetylation might exist^{36–38}.

In support of a direct inhibition of HAT activity by polyamines, $\Delta iki3\Delta sas3$ cells responded significantly less well to the lifespan-extending effect of spermidine, compared with wild-type cells (Fig. 5b, $P < 0.001$). Accordingly, depletion of polyamines by deletion of *SPE1* in this background ($\Delta spe1\Delta iki3\Delta sas3$) did not diminish survival to the same level as *SPE1* deletion did in wild-type cells (*Δspe1*; Supplementary Information, Fig. S6a, b). Again, this suggests that ageing-related HAT activity acts downstream of polyamines.

Spermidine treatment induces autophagy in all model systems tested

As histone modifications are pivotal for the control of gene transcription, we performed microarray analyses of spermidine-aged cells. Several (macro)autophagy-related genes (most significantly *ATG7*) were upregulated after spermidine treatment (Fig. 5e, f; Supplementary Information, Table S2). The results were verified for three of these genes (*ATG7*, *11* and *15*) by quantitative reverse transcription real-time PCR (Fig. 5g). In addition, chromatin immunoprecipitation (ChIP) analysis using an antibody against acetylated Lys 18 of histone H3 revealed that the promoter region of *ATG7* (*pATG7*) was maintained at a higher acetylation status, compared with six out of seven adjacent promoter regions (Fig. 5h) during the physiological course of ageing. The specific hyperacetylation of *pATG7* was significantly enhanced by treatment with spermidine (Fig. 5h), which could be the cause, or at least a prerequisite, for the observed increase in *ATG* mRNAs in spermidine-aged cells. These results suggest that during chronological ageing of yeast cells, which is accompanied by general deacetylation of histone H3, certain classes of genes (such as *ATG* genes) are protected from strong hypoacetylation, thus maintaining accessibility of the promoter region and allowing for their transcription.

Autophagy is believed to be essential for healthy ageing and longevity, and the autophagy-regulatory Tor-pathway constitutes one of the three highly conserved age-controlling signalling pathways^{14–16}. To test whether spermidine treatment resulted in enhanced autophagy, we monitored the subcellular localization of Atg8p, which translocates to autophagosomes as a typical sign of macroautophagy. Control cells showed a diffuse distribution of the EGFP-Atg8p fusion protein, whereas spermidine-treated cells manifested clear vacuolar localization of EGFP-Atg8p in an *ATG7*-dependent manner (Fig. 6a; Supplementary

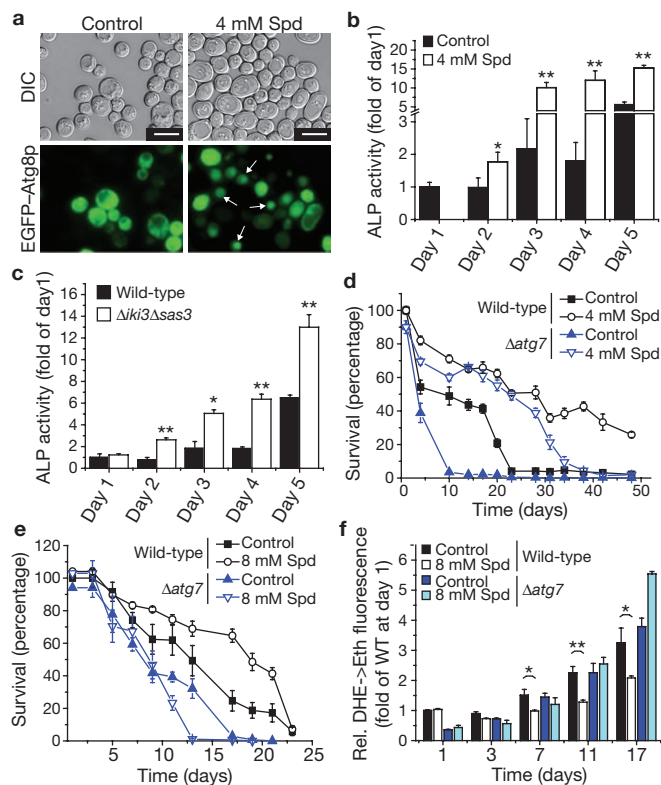


Figure 6 Autophagy is induced by spermidine and critical for maximal life span extension in yeast. (a) Fluorescence microscopy of wild-type yeast cells expressing an EGFP-Atg8p fusion protein with or without (control) treatment of 4 mM spermidine for 48 h. White arrows indicate vacuolar localization of EGFP-Atg8p indicative of autophagy. Scale bars, 5 μ m. (b) Relative alkaline phosphatase activity (ALP activity) indicative of autophagy during chronological ageing of *pho8 Δ C60* yeast with (open bars) or without (closed bars) application of spermidine (4 mM). Data represent means \pm s.e.m. ($n = 3$; * $P < 0.01$ and ** $P < 0.001$). (c) Relative alkaline phosphatase activity (ALP activity) indicative of autophagy during chronological ageing of wild-type (closed bars) and $\Delta iki3\Delta sas3$ (open bars) cells. Data represent means \pm s.e.m. ($n = 3$; * $P < 0.01$ and ** $P < 0.001$). (d) Chronological ageing of wild-type (\blacksquare , \circ) and $\Delta atg7$ (\blacktriangledown , \blacktriangledown) with (open symbols) or without (closed symbols) addition of spermidine (4 mM) at day 1. Data represent means \pm s.e.m. ($n = 4$). (e) Chronological ageing on water of wild-type (\blacksquare , \circ) and $\Delta atg7$ (\blacktriangledown , \blacktriangledown) with (open symbols) or without (closed symbols) addition of spermidine (8 mM) at day 0. Data represent means \pm s.e.m. ($n = 4$). (f) Quantification (fluorescence reader) of ROS production (DHE \rightarrow Eth conversion) by wild-type and $\Delta atg7$ cells with and without supplementation of spermidine (8 mM), obtained from the ageing experiment shown in panel e. Data represent means \pm s.e.m. ($n = 4$; * $P < 0.07$ and ** $P < 0.01$).

Information, Fig. S6c, d). We also indirectly quantified the induction of autophagy during the progress of chronological ageing by assessing the activity of alkaline phosphatase (ALP). Addition of spermidine enhanced ALP activity up to 5-fold (Fig. 6b). Similarly, ALP activity increased up to 3-fold during early ageing in cells deleted of *IKI3* and *SAS3* (Fig. 6c), consistent with the hypothesis that modulation of HAT activity directly regulates autophagy.

Spermidine also induced autophagy in cultured human cells (Fig. 7a, b) and in flies (Fig. 7c, d). HeLa cells treated with spermidine (100 μ M) for 6 h showed a clear relocalization of LC3-GFP (the mammalian orthologue of Atg8p) into cytoplasmic puncta (Fig. 7a, b). Immunoblot detection of accumulating LC3-II, the lipidated, autophagosome-associated form of LC3, confirmed induction of autophagy by spermidine in these

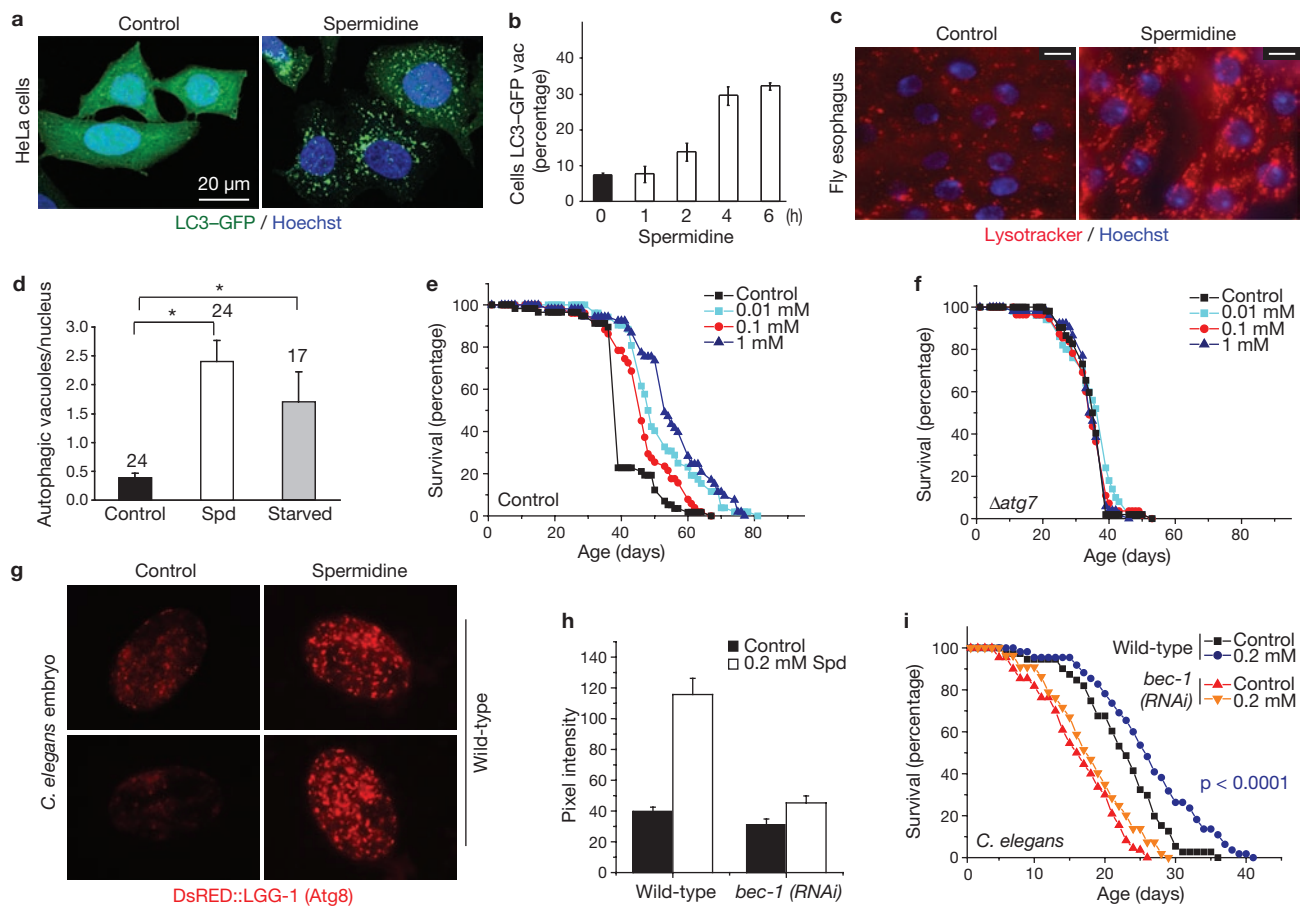


Figure 7 Autophagy is essential for spermidine-induced life span extension in flies and worms. **(a)** Fluorescence microscopy of Hoechst-counterstained HeLa cells transiently transfected with LC3-GFP subjected to 100 μ M spermidine for 6 h. Representative pictures are shown. **(b)** Percentage of adherent cells exhibiting a clear LC3-GFP relocalization into cytoplasmic vacuoles. Numbers were determined using micrographs of Hoechst-counterstained HeLa cells as representatively shown in **a**. Data represent means \pm s.d. ($n = 3$). **(c)** LysoTracker Red staining of vacuoles indicative of autophagy in oesophagus tissue from flies fed with 1 mM spermidine for two days, compared with controls (without spermidine). Nuclei were visualized by Hoechst staining. Scale bars, 10 μ m. **(d)** Quantification of autophagic vesicles per nucleus in LysoTracker Red stained muscle tissue of female flies fed with supplementation of 1 mM spermidine or with 10% glucose (starved) for 48 h, compared with normal food (control). Data represent means \pm s.e.m. of at least 20 flies for each group ($*P < 0.01$). **(e, f)** Survival of *Drosophila* during ageing without (control) and with supplementation of food at various concentrations

of spermidine (as indicated). Autophagy-deficient flies **(f)** homozygous mutant for *Atg7* ($\Delta atg7$) were compared with flies capable of autophagy **(e)** and heterozygous for *Atg7* (control). For details of strains and additional wild-type controls, see Supplementary Information Methods and Fig. S6h, i. **(g)** Fluorescence microscopy of *C. elegans* transgenic embryos expressing a full-length p_{DsRED} ::DsRED::LGG-1 fusion protein indicative of autophagic activity. Shown are two representative pictures of embryos untreated (control) or treated with spermidine (0.2 mM) supplementation of food. **(h)** Quantification of autophagic activity through measurement of DsRED::LGG-1 pixel intensity from images of wild-type animals shown in **g**, and *bec-1* RNAi knockdown animals (*bec-1* RNAi). Data represent means \pm s.e.m. ($n = 3$) with at least 25 images processed for each trial. **(i)** Survival of *C. elegans* during ageing with and without (control) supplementation of food (UV-killed *E. coli*) with spermidine (0.2 mM). Wild-type (N2) animals were compared with *bec-1* RNAi animals deficient in autophagy induction. For mean life spans see Supplementary Information, Table S3.

cells (Fig. S6f, g). The oesophagus of flies fed with spermidine (1 mM) for 48 h showed an increase in the number of LysoTracker Red-positive vacuoles, indicating increased autophagy, which even exceeded that of starved flies (Fig. 7c, d). Finally, nematodes that were grown on spermidine-rich medium showed cytoplasmic aggregation of the DsRed::LGG3 fusion protein (LGG3 is the *C. elegans* orthologue of Atg8), indicating autophagy (Fig. 7g, h). Together, these results indicate that spermidine induces autophagy in cells of yeasts, flies, nematodes and mammals.

Autophagy is required for spermidine-mediated lifespan extension in yeast, flies and worms

Autophagy has been suggested to play an important part in various models of longevity^{39–41}. We therefore asked whether the observed

enhancement of autophagy is essential for the lifespan-extending effects of spermidine. Consistent with this possibility, deletion of *ATG7* compromised the lifespan-extending effects of spermidine application in yeast (Fig. 6d, e). Although survival could be protracted by spermidine early during ageing (indicating ‘backup’ mechanisms), *atg7* mutant cells treated with spermidine lost viability after about 30 days of ageing (Fig. 6d; Supplementary Information Results and Discussion). However, when aged in water, spermidine extended the lifespan of yeast cells in a highly *ATG7*-dependent manner throughout the entire ageing process (Fig. 6e, f). Spermidine enhanced survival by up to 3-fold ($P < 0.0001$) and also significantly reduced ROS levels ($P < 0.0001$) in wild-type cells. By contrast, spermidine failed to improve survival or to reduce ROS in *atg7* mutant

cells (Fig. 6e, f). Similarly, homozygous deletion of *ATG7* completely abrogated spermidine-induced lifespan extension in flies (Fig. 7e, f; see Supplementary Information, Fig. S6h, i for mean lifespans and *P* values). Knockdown of *Beclin-1*, yet another essential autophagy gene homologous to yeast *ATG6*, abolished the spermidine-mediated increase in lifespan of *C. elegans* (Fig. 7i). In conclusion, autophagy is crucial for polyamine-mediated lifespan extension, in yeast, flies and nematodes.

DISCUSSION

Here, we report the discovery that endogenous and exogenous levels of spermidine induce autophagy, which in turn increases lifespan in a variety of model organisms. Studies have suggested that induction of autophagy might be useful for the treatment of bacterial and viral infections⁴² as well as that of cancer^{43–45}, and it remains to be seen whether spermidine-induced autophagy might be therapeutically useful beyond its anti-ageing effects.

Beside its pro-autophagic effect, spermidine was found to suppress several ageing-associated laboratory parameters, such as overproduction of ROS and the level of necrotic cell death. Autophagy constitutes the major lysosomal degradation pathway for recycling damaged and potentially harmful cellular material (for example, defective mitochondria). Of note, autophagy counteracts cell death and prolongs lifespan in various models of ageing^{17,18,40}. Therefore, inhibition of cell death by autophagy could facilitate the long-term survival of spermidine-treated cells and organisms.

Ageing-associated necrotic death can be inhibited by simply adding spermidine to yeast and human immune cells or by genetic modification of the HAT machinery in yeast, arguing in favour of programmed rather than accidental necrotic death. Necrotic cell death culminates in the leakage of intracellular compounds resulting in local inflammation, which in turn is suspected to cause ageing ('inflammaging'). A recent study proposed that chronic inflammation might be one of the driving forces of human ageing, causing immunosenescence⁴⁶. In support of this theory, we showed that spermidine potently inhibits necrotic death of ageing human PBMC and protects mice from oxidative stress in the serum. Thus, programmed necrotic processes might be of cardinal importance in understanding the mechanisms of organismal ageing in general.

Mechanisms that account for the cytoprotective autophagy induction by spermidine have been elucidated to some extent in yeast. Our data are compatible with a model in which spermidine inhibits the activity of HATs (such as Iki3p and Sas3p), causing histone H3 hypoacetylation, which in turn affects the epigenetic regulation of gene transcription, allowing for the induction of autophagy-relevant transcripts. Global hypoacetylation of histones indicates silencing of the majority of genes that might be important for saving resources on specific pro-survival processes (e.g. autophagy). Indeed, our results argue in favour of selective mechanisms that protect certain classes of genes (e.g. *ATG* genes) from strong deacetylation during ageing, thereby allowing their transcription. However, at this point, we do not know whether the (de)acetylation of histones, as opposed to non-histone proteins (other HAT substrates such as tubulin), fully explain the anti-ageing potential of spermidine. The hypothesis that regulation of HAT activity (in addition to that of deacetylases) might contribute to the regulation of ageing remains to be investigated in close detail.

Importantly, polyamine concentrations, as well as autophagy, decline during ageing of various organisms, including humans^{19,47}. Here we show that external supplementation of spermidine prolongs lifespan in yeast, flies, nematodes and human immune cells. Future studies will tell whether spermidine, its derivatives, or agents that affect polyamine biosynthesis and degradation might have beneficial effects on human health. □

METHODS

Methods and any associated references are available in the online version of the paper at <http://www.nature.com/naturecellbiology/>

Note: Supplementary Information is available on the Nature Cell Biology website.

ACKNOWLEDGMENTS

We thank Ulrike Potocnik, Silvia Dichtinger, Arno Absenger and Elfgard Heintz for assistance. We are grateful to the Austrian Science Fund FWF (Austria) for grant S-9304-B05 (to F.M., S.B. and D.C.-G.), grant S-9303-B05 (to K.-U.F. and H.K.), grant LIPOTOX (to F.M. and S.B.), and grant S-9301-B05 (to B.G.-L.) and to the European Commission for project TransDeath (to K.-U.F. and C.R.), project APOSYS (to F.M., T.E. and G.K.) and project Lifespan (FP6 036894 to B.G.-L.). We are grateful to the Austrian Science Fund FWF (Vienna, Austria) for grants S9302-B05 (to M.B.) and to the European Commission (Brussels, Europe) for project MIMAGE (contract no. 512020; to M.B.).

AUTHOR CONTRIBUTIONS

T.E., G.K. and F.M. designed and organized this study and wrote the manuscript. T.E. performed the largest part of the yeast and mouse experiments and contributed significantly to the fly and PBMC cell culture data. H.K., A.S., S.B., C.R., D.C.-G., J.R., S.S., H.F., L.A. and B.A. contributed to the yeast experiments. C.M. and F.S. performed polyamine measurements by MassSpec. L.D., R.H. and N.M. performed the fly experiments. E.S. contributed to mouse data. A.C. performed HELA cell culture experiments. E.M. and N.T. contributed the worm data. D.W. and B.G.-L. performed PBMC experiments. P.L., G.H. and M.B. determined yeast replicative life spans. N.M., E.H., K.-U.F., S.B., C.R. and D.C.-G. contributed with decisive discussions and helped to design experiments.

COMPETING FINANCIAL INTERESTS

The authors declare competing financial interests: a patent application including data from this article has been filed.

Published online at <http://www.nature.com/naturecellbiology/>

Reprints and permissions information is available online at <http://npg.nature.com/reprintsandpermissions/>

- Fabrizio, P. *et al.* Superoxide is a mediator of an altruistic aging program in *Saccharomyces cerevisiae*. *J. Cell Biol.* **166**, 1055–1067 (2004).
- Herker, E. *et al.* Chronological aging leads to apoptosis in yeast. *J. Cell Biol.* **164**, 501–507 (2004).
- Vicencio, J. M. *et al.* Senescence, apoptosis or autophagy? When a damaged cell must decide its path—a mini-review. *Gerontology* **54**, 92–99 (2008).
- Golstein, P. & Kroemer, G. Cell death by necrosis: towards a molecular definition. *Trends Biochem. Sci.* **32**, 37–43 (2007).
- Zong, W. X. & Thompson, C. B. Necrotic death as a cell fate. *Genes Dev.* **20**, 1–15 (2006).
- Imai, S., Armstrong, C. M., Kaerberlein, M. & Guarente, L. Transcriptional silencing and longevity protein Sir2 is an NAD-dependent histone deacetylase. *Nature* **403**, 795–800 (2000).
- Lin, S. J., Defossez, P. A. & Guarente, L. Requirement of NAD and SIR2 for life-span extension by calorie restriction in *Saccharomyces cerevisiae*. *Science* **289**, 2126–2128 (2000).
- Lamming, D. W. *et al.* HST2 mediates SIR2-independent life-span extension by calorie restriction. *Science* **309**, 1861–1864 (2005).
- Jenuwein, T. & Allis, C. D. Translating the histone code. *Science* **293**, 1074–1080 (2001).
- Kaerberlein, M., Burtner, C. R. & Kennedy, B. K. Recent developments in yeast aging. *PLoS Genet.* **3**, e84 (2007).
- Longo, V. D. & Kennedy, B. K. Sirtuins in aging and age-related disease. *Cell* **126**, 257–268 (2006).
- Dang, W. *et al.* Histone H4 lysine 16 acetylation regulates cellular lifespan. *Nature* **459**, 802–807 (2009).
- Longo, V. D. & Finch, C. E. Evolutionary medicine: from dwarf model systems to healthy centenarians? *Science* **299**, 1342–1346 (2003).
- Powers, R. W., 3rd, Kaerberlein, M., Caldwell, S. D., Kennedy, B. K. & Fields, S. Extension of chronological life span in yeast by decreased TOR pathway signaling. *Genes Dev.* **20**, 174–184 (2006).

15. Bonawitz, N. D., Chatenay-Lapointe, M., Pan, Y. & Shadel, G. S. Reduced TOR signaling extends chronological life span via increased respiration and upregulation of mitochondrial gene expression. *Cell Metab.* **5**, 265–277 (2007).
16. Harrison, D. E. *et al.* Rapamycin fed late in life extends lifespan in genetically heterogeneous mice. *Nature* **460**, 392–395 (2009).
17. Galluzzi, L. *et al.* To die or not to die: that is the autophagic question. *Curr. Mol. Med.* **8**, 78–91 (2008).
18. Jia, K. & Levine, B. Autophagy is required for dietary restriction-mediated life span extension in *C. elegans*. *Autophagy* **3**, 597–599 (2007).
19. Scalabrino, G. & Ferioli, M. E. Polyamines in mammalian ageing: an oncological problem, too? A review. *Mech. Ageing Dev.* **26**, 149–164 (1984).
20. Weinberger, M. *et al.* Apoptosis in budding yeast caused by defects in initiation of DNA replication. *J. Cell Sci.* **118**, 3543–3553 (2005).
21. Allen, C. *et al.* Isolation of quiescent and nonquiescent cells from yeast stationary-phase cultures. *J. Cell Biol.* **174**, 89–100 (2006).
22. Laun, P. *et al.* Aged mother cells of *Saccharomyces cerevisiae* show markers of oxidative stress and apoptosis. *Mol. Microbiol.* **39**, 1166–1173 (2001).
23. Fabrizio, P., Pozza, F., Pletcher, S. D., Gendron, C. M. & Longo, V. D. Regulation of longevity and stress resistance by Sch9 in yeast. *Science* **292**, 288–290 (2001).
24. Harman, D. Aging: a theory based on free radical and radiation chemistry. *J. Gerontol.* **11**, 298–300 (1956).
25. Schraml, E. *et al.* Norepinephrine treatment and aging lead to systemic and intracellular oxidative stress in rats. *Exp. Gerontol.* **42**, 1072–1078 (2007).
26. Artal-Sanz, M., Samara, C., Syntichaki, P. & Tavernarakis, N. Lysosomal biogenesis and function is critical for necrotic cell death in *Caenorhabditis elegans*. *J. Cell Biol.* **173**, 231–239 (2006).
27. Syntichaki, P., Samara, C. & Tavernarakis, N. The vacuolar H⁺-ATPase mediates intracellular acidification required for neurodegeneration in *C. elegans*. *Curr. Biol.* **15**, 1249–1254 (2005).
28. Burtner, C. R., Murakami, C. J., Kennedy, B. K. & Kaeblerlein, M. A molecular mechanism of chronological aging in yeast. *Cell Cycle* **8**, 1256–1270 (2009).
29. Fabrizio, P. *et al.* Sir2 blocks extreme life-span extension. *Cell* **123**, 655–667 (2005).
30. Burhans, W. C. & Weinberger, M. Acetic acid effects on aging in budding yeast: Are they relevant to aging in higher eukaryotes? *Cell Cycle* **8** (2009).
31. Scaffidi, P., Misteli, T. & Bianchi, M. E. Release of chromatin protein HMGB1 by necrotic cells triggers inflammation. *Nature* **418**, 191–195 (2002).
32. Weinberger, M. *et al.* DNA replication stress is a determinant of chronological lifespan in budding yeast. *PLoS ONE* **2**, e748 (2007).
33. Duncan, E. M. *et al.* Cathepsin L proteolytically processes histone H3 during mouse embryonic stem cell differentiation. *Cell* **135**, 284–294 (2008).
34. Howe, L. *et al.* Histone H3 specific acetyltransferases are essential for cell cycle progression. *Genes Dev.* **15**, 3144–3154 (2001).
35. Winkler, G. S., Kristjuhan, A., Erdjument-Bromage, H., Tempst, P. & Svejstrup, J. Q. Elongator is a histone H3 and H4 acetyltransferase important for normal histone acetylation levels *in vivo*. *Proc. Natl Acad. Sci. USA* **99**, 3517–3522 (2002).
36. Hobbs, C. A., Paul, B. A. & Gilmour, S. K. Elevated levels of polyamines alter chromatin in murine skin and tumors without global changes in nucleosome acetylation. *Exp. Cell Res.* **290**, 427–436 (2003).
37. Hobbs, C. A., Paul, B. A. & Gilmour, S. K. Deregulation of polyamine biosynthesis alters intrinsic histone acetyltransferase and deacetylase activities in murine skin and tumors. *Cancer Res.* **62**, 67–74 (2002).
38. Liu, B., Sutton, A. & Sternglanz, R. A yeast polyamine acetyltransferase. *J. Biol. Chem.* **280**, 16659–16664 (2005).
39. Juhasz, G., Erdi, B., Sass, M. & Neufeld, T. P. Atg7-dependent autophagy promotes neuronal health, stress tolerance, and longevity but is dispensable for metamorphosis in *Drosophila*. *Genes Dev.* **21**, 3061–3066 (2007).
40. Tavernarakis, N., Pasparaki, A., Tasdemir, E., Maiuri, M. C. & Kroemer, G. The effects of p53 on whole organism longevity are mediated by autophagy. *Autophagy* **4**, 870–873 (2008).
41. Melendez, A. *et al.* Autophagy genes are essential for dauer development and life-span extension in *C. elegans*. *Science* **301**, 1387–1391 (2003).
42. Orvedahl, A. & Levine, B. Eating the enemy within: autophagy in infectious diseases. *Cell Death Differ.* **16**, 57–69 (2009).
43. Hoyer-Hansen, M. & Jaattela, M. Autophagy: an emerging target for cancer therapy. *Autophagy* **4**, 574–580 (2008).
44. Lambert, L. A. *et al.* Autophagy: a novel mechanism of synergistic cytotoxicity between doxorubicin and roscovitine in a sarcoma model. *Cancer Res.* **68**, 7966–7974 (2008).
45. Lefranc, F., Facchini, V. & Kiss, R. Proautophagic drugs: a novel means to combat apoptosis-resistant cancers, with a special emphasis on glioblastomas. *Oncologist* **12**, 1395–1403 (2007).
46. Franceschi, C. *et al.* Inflammaging and anti-inflammaging: a systemic perspective on aging and longevity emerged from studies in humans. *Mech. Ageing Dev.* **128**, 92–105 (2007).
47. Levine, B. & Kroemer, G. Autophagy in the pathogenesis of disease. *Cell* **132**, 27–42 (2008).

METHODS

Yeast strains and molecular biology. Experiments were carried out in BY4741 (MATA *his3Δ1 leu2Δ0 met15Δ0 ura3Δ0*) and respective null mutants, obtained from Euroscarf. Strains were grown at 28 °C on SC medium containing 0.17% yeast nitrogen base (Difco), 0.5% (NH₄)₂SO₄ and 30 mg l⁻¹ of all amino acids (except histidine, 80 mg l⁻¹ and leucine, 200 mg l⁻¹), 30 mg l⁻¹ adenine and 320 mg l⁻¹ uracil with 2% glucose (SCD). To demonstrate the complete requirement of polyamines for lifespan extension on media alkalization, experiments were carried out in polyamine-free SCD, obtained by sterile filtering and special treatment of glass ware as described⁴⁸.

Plasmid construction and yeast knockout generation. *Spe1* double-mutant strains (with *yca1*, *mma111*, *aif1*, *nuc1*) were obtained through mating and sporulation of BY4741 *Δspe1* with the respective BY4742 (Mata) single mutant strains. Single and double-mutant strains were verified for correct gene deletion by PCR with primers listed in Supplementary Information, Table S4 and further checked for consistent auxotrophies. The double mutant *Δiki3Δsas3* was generated according to previous methods⁴⁹ by using a gene-specific URA3-knockout cassette, amplified by PCR with pUG72 as a template. Primers are listed in Supplementary Information, Table S4. The double-mutant phenotype was confirmed using a strain generated by mating and sporulation of the respective single mutants (BY4742 *Δiki3* MATA and BY4741 *Δsas3* MATA). The *SPE1*, *IKI3* and *SAS3* triple mutant (*Δspe1Δiki3Δsas3*) was obtained by targeted deletion of *SPE1* using pUG73 as template in the background of *Δiki3Δsas3* resulting in the following genotype: BY4741 *spe1::LEU2 iki3::URA3 sas3::kanMX*.

On deletion of both *IKI3* and *SAS3*, we observed slight aggregation of cells possibly because of a defect in late budding events. For calculation of survival rates in experiments using *Δiki3Δsas3*, therefore, cell numbers of each sample were determined after two pulses of sonication on ice with Sonifier 250 from Benson (Duty Cycle: 35; Output Control: 2.5). Notably, at least three different clones of each generated mutant were tested for the survival plating during ageing to rule out clonal variation.

To construct *NHP6A*-EGFP in pUG35-Ura (giving rise to a C-terminally tagged chimaeric fusion protein under the control of the met25-Promotor) the insert was amplified by PCR using genomic DNA from BY4741 as a template and cloned into pUG35 using the *EcoRI* restriction site. The EGFP-*ATG8* construct in pUG36-Ura (N-terminally tagged fusion protein) was similarly generated, using *EcoRI* and *Clal* restriction sites. Primers are listed in Supplementary Information, Table S4.

Yeast survival plating. For chronological ageing experiments, cultures were inoculated from fresh overnight cultures to an absorbance of 0.1 (~1.10⁶ cells ml⁻¹) at a culture volume of 10% of flask volume. Aliquots were taken out to perform survival plating at indicated time points². Survival of wild-type control cultures at day 1 was set to 100% and other samples calculated accordingly. If not otherwise stated, representative ageing experiments are shown with at least three independent samples (as indicated) aged at the same time. Experiments have been performed at least three times in total with similar outcome. As polyamines are required for normal growth of yeast⁴⁸, experimental conditions for chronological ageing of *Δspe1* (Fig. 2, Supplementary Information, Figs S3b, S6a, b) were adapted in a way that *Δspe1* cells still retained sufficient polyamine concentrations when growing, but showed maximal attenuation of intracellular polyamines upon entry into stationary phase, where chronological ageing begins (for details see Supplementary Information, Results and Discussion).

Spermidine-free base (S4139, Sigma) was added to stationary cultures at day 1 of the ageing experiments (24 h after inoculation). For complementation of *Δspe1* phenotypes spermidine or putrescine (P5780, Sigma) were added to medium before inoculation to a final concentration of 0.1 mM. Aqueous stock solution of spermidine (1 M) was stored in single-use aliquots at -20 °C for no longer than 1 month. For adjustment of extracellular pH (pH_{ex}) to 6 (± 0.5), the required amount of sodium hydroxide was added 30 h after inoculation. The pH_{ex} was repeatedly adjusted at approximately 6 (± 0.5) throughout the ageing process.

Yeast ageing on water was performed by transferring stationary cultures (30 h after inoculation) to sterile double-distilled water and repeating the process after every four days of ageing. In this case, spermidine (8 mM, final concentration) was added to growth medium before inoculation and the pH was closely titrated to control conditions (pH ~ 4.5) using hydrochloric acid. Note that medium

supplementation with valine (8 mM) and ammonium sulphate (16 mM), used as an additional control to exclude a simple feeding effect of spermidine, showed no effect on survival and ROS production (data not shown).

Test for cell death markers in yeast. Tests for apoptotic (TUNEL and annexin V staining) and necrotic (PI staining) markers, as well as markers for oxidative stress (DHE staining), were performed as described previously⁵⁰. For quantifications using flow cytometry (BD FACSAria), 30,000 cells were evaluated and analysed with BD FACSDiva software.

As a further marker for necrosis, nuclear release of the yeast HMGB1 homologue (Nhp6Ap) was monitored by epifluorescence microscopy of the ectopically expressed chimaeric fusion protein, Nhp6Ap-EGFP. Therefore, yeast strains transformed with pUG35/*NHP6A* were grown on SCD lacking uracil and aged until the indicated time-points. Cells were washed once with PBS and applied to epifluorescence microscopy directly with the use of small-band EGFP filter (Zeiss) on a Zeiss Axioskop microscope to monitor intracellular localization of Nhp6A-EGFP. Expression during ageing was verified by immunoblotting (data not shown). Notably, release of Nhp6A-EGFP to the extracellular space, reported for mammalian HMGB1⁵¹, could not be detected in yeast after 100× concentration of culture medium (data not shown).

Yeast autophagy measurements. Autophagy was monitored either by vacuolar localization of Atg8p using fluorescence microscopy of cells expressing an EGFP-Atg8 fusion protein⁵² or by alkaline phosphatase (ALP) activity according to published methods⁵³ using BY4741 wild-type or *Δiki3Δsas3* cells transformed with and selected for stable insertion of pTN9 *HindIII* fragment (confirmed by PCR). To correct for intrinsic (background) ALP activity, BY4741 (without pTN9) had been simultaneously processed and ALP activity subtracted. For generation of EGFP-*ATG8* constructs see section on Molecular Biology.

Yeast replicative life span determination. For replicative lifespan analysis of BY4741 synthetic complete glucose medium (SC-glucose) containing 2% (w/v) D-glucose, 0.17% yeast nitrogen base (Difco), 0.5% (NH₄)₂SO₄ and 10 ml complete dropout was used. Complete dropout contains: 0.2% Arg, 0.1% His, 0.6% Ile, 0.6% Leu, 0.4% Lys, 0.1% Met, 0.6% Phe, 0.5% Thr, 0.4% Trp, 0.1% Ade, 0.4% Ura, 0.5% Tyr. Agar plates were made by adding 2% (w/v) agar to the medium. Where necessary, spermidine from a freshly prepared aqueous stock solution (0.2 M, pH 7.0) was added to a final concentration of 1 mM. Pre-tests showed that this concentration does not influence growth properties of fraction V cells (data not shown). Preparation of senescent yeast cells (fraction V) by elutriation was performed as described previously²². To determine the remaining lifespan of fraction II and fraction V cells, cohorts of 80 randomly chosen cells per fraction were taken directly after elutriation and, for each cell, the number of remaining cell cycles was determined by micromanipulation. Cells that never budded were excluded from the analysis. Statistical analysis was performed as described previously²².

Drosophila lifespan experiments. Flies from an isogenized w¹¹¹⁸ strain were used in all the experiments. They were kept in a 25 °C, 70% humidity, 12 h light/ 12 h dark incubator. Spermidine (S4139, Sigma) was prepared as a 1 M stock solution in sterile distilled water, aliquoted in single-use portions and stored at -20 °C. New stock solution was prepared once a month. Spermidine was mixed to liquid food medium (2.2% sugar beet syrup, 8% malt extract, 1.8% yeast, 1.2% nipagine). In a preliminary experiment, we checked that the flies ate normally when fed with spermidine-supplemented food to exclude a dietary restriction effect on lifespan. Food colorant was added to normal food and the food mixed with 10 μM, 100 μM, 1 mM or 10 mM spermidine. The intensity of the colour in the flies' abdomens was checked regularly for 24 h. We could not detect any difference between the control group and the groups fed spermidine at all concentrations.

A total of 60 newly eclosed flies were collected in each group. Both males and females were studied. Twenty flies of the same sex were put in an empty vial closed with a foam plug in which a cut was made to insert a filter paper soaked with 400 μl of food. The filters were replaced by new ones and dead flies were counted every weekday. Over the weekend, 1.2 ml of food was given to the flies. Comparison of survivorship data was performed using log rank and Wilcoxon survival tests and corrected for multiple comparisons against the control group. Each sex and replicate was analysed separately.

The lines for the generation of *Atg7[±]* and *Atg7^{-/-}* flies were kindly provided by T. Neufeld (University of Minnesota, USA)³⁹. The homozygote mutants, *Atg7^{d14}*/*Atg7^{d14}* are homozygous mutants for *Atg7*, heterozygous for *Sec6* and *CG5335*. The flies of the genotype *CG5335^{d30}*/*Atg7^{d14}* (heterozygous for *Atg7*, *Sec6* and *CG5335*) were used as controls. For life span experiments of *Atg7* mutants, an *yw* control (obtained from The Bloomington Stock Center, Indiana, USA) was included as the closest genetic background for the *Atg7* lines. Similar results were obtained as compared to *CG5335^{d30}*/*Atg7^{d14}* flies (see Supplementary Information, Fig. S6h, i for mean lifespans).

Autophagy measurements in *Drosophila* tissue. *W¹¹¹⁸* females were kept for 48 h on normal food (control), food supplemented with 1 mM spermidine (spermidine) or on a 10% glucose solution (starved). Muscles from the thorax and sections of the oesophagus were dissected in PBS and then transferred for 2 min in a PBS solution containing the fluorescent dyes Hoechst 4,432 (dilution 1:1000) and LysoTracker Red DND-99 (Invitrogen, Ref L7528) diluted 1:10000. After staining, the tissues were transferred on a microscope slide (SuperFrost UltraPlus Menzel-Gläser Nr. J4800AMNZ), covered with a coverslip and immediately imaged with a fluorescence microscope Zeiss axioplan 2 imaging / Coolsnap HQ. At least 20 flies were imaged for each group. On each picture from the muscles, the number of autophagic vesicles recognized by the LysoTracker dye and the nuclei were manually counted. The ratio of vesicles to nuclei was calculated for each picture and analysed with a Kruskal-Wallis test corrected with a Bonferroni post hoc tests.

Blood samples, preparation and culture of peripheral blood mononuclear cells (PBMC). Peripheral full blood (60 ml) was obtained from healthy young (<35 years) persons, registered at the Institute for Biomedical Ageing Research as blood donors. Informed written consent was obtained and the study was approved by the local ethics committee. PBMCs were purified from heparinized blood by Ficoll Paque density gradient centrifugation (Pharmacia). PBMCs were cultured for 12 days in RPMI 1640 (Life Technologies) supplemented with 10% fetal calf serum (Sigma-Aldrich), 1% penicillin-streptomycin (Gibco, Invitrogen Corporation) and phytohemagglutinin (PHA) (1 µg ml⁻¹; Sigma) using 24-well plates (BD) for 12 days. PBMCs were kept at a density of 10⁶ cells per well at 37 °C, 5% CO₂. Spermidine (Sigma) was added after 1 and 7 days of culture (0 nM, 0.2 nM, 2 nM, 20 nM and 2 µM). Survival of cells was measured after 6 and 12 days.

Immunofluorescence staining of PBMCs. Cells were washed (500g, 10 min, room temperature) with phosphate buffered saline (PBS) and resuspended in 50 µl PBS per 10⁶ cells. Necrosis staining of cells was performed by adding the DNA intercalator 7-aminoactinomycin D (7-AAD), which is visible in the Phycoerythrin (PE) channel, at a concentration of 0.5 µl 50 µl⁻¹ PBS and incubated for 30 min at 4 °C. Cells were then washed with PBS and resuspended in 100 µl annexin binding buffer (10 mM HEPES, 140 mM NaCl, 2.5 mM CaCl₂ pH 7.4). Fluorescein isothiocyanate (FITC)-labelled annexin V (5 µl; BD Pharmingen) was added and samples were incubated for 15 min at room temperature in the dark. Finally, annexin-binding buffer (400 µl) was added, samples were kept on ice and measured at the FACS immediately. Cells which were negative for both staining were considered as viable⁵⁴.

HeLa cell culture conditions, plasmid transfection and autophagy measurements. HeLa cells were cultured in Dulbecco's modified Eagle's medium (DMEM) containing 10% fetal calf serum (FCS), 1 mM pyruvate and 10 mM Hepes at 37 °C under 5% CO₂. For plasmid transfection cells were cultured in six-well plates and transfected at 80% confluence. Transient transfections with LC3-GFP plasmid were performed with Lipofectamine 2000 reagent (Invitrogen) and cells were used 24 h after transfection. For fluorescence microscopy, HeLa cells transfected with LC3-GFP were fixed with paraformaldehyde (4%, w/v) and nuclei were labelled with 10 mg ml⁻¹ Hoechst 33,342 (Molecular Probes-Invitrogen). Fluorescence microscopy was analysed with a Leica IRE2 equipped with a DC300F camera. For western blot analysis, cells were washed with cold PBS at 4 °C and lysed as described previously⁵⁵. Protein (50 µg) was loaded on a 10% SDS-PAGE precasted gel (Invitrogen) and transferred to Immobilon membrane (Millipore). The membrane was incubated for 1 h in TBS-Tween 20 (0.05%) containing 5% nonfat milk. Primary antibodies including anti-LC3 I/II (Cell Signaling) were incubated overnight at 4 °C and visualized with the appropriate horseradish peroxidase-labelled secondary antibodies (Southern Biotechnologies Associates) plus the SuperSignal

West Pico chemoluminescent substrate (Pierce). Anti-GAPDH (Chemicon) antibody was used to control equal loading.

Experimental animals and determination of thiol groups in mice serum. Male and female C57BL/6 mice were purchased from the Institut für Labortierkunde und Genetik, Himberg, Austria. Treatment of animals started at an age between 12 and 16 weeks. All mice were kept and treated according to institutional guidelines and Austrian law and the experiments were approved by the responsible governmental commission. For each group, one male and two female mice were housed singly and fed *ad libitum* with regular food (pellets) and spermidine was added to drinking water at concentrations of 0.3 and 3 mM for 200 days. Control mice were given pure drinking water. Drinking water was replaced every 2–3 days and spermidine freshly added from 1 M aqueous stock (spermidine/HCl pH 7.4), which was kept at –20 °C for no longer than one month. Food and body weight, calculated on a weekly basis, remained unaffected by supplementation of spermidine (data not shown), indicating that not calorie restriction could account for the observed effects. At the end of the experiment, the animals were anaesthetized by ether inhalation, and exsanguinated by heart puncture. Peripheral blood was allowed to clot for 20 min and serum was obtained by centrifugation at 200g for 10 min. The spleens and livers (shock frozen in liquid nitrogen and stored at –80 °C until further use) were immediately excised. Serum was used for determination of free thiol groups by Ellman's reaction^{56,57} as described previously²⁵. Spleen weight, which was similar in all groups, indicated that all mice were of similar general health (data not shown).

***C. elegans* life span analysis.** We followed standard procedures for *C. elegans* strain⁵⁸. Nematode rearing temperature was kept at 20 °C. The N2, wild-type Bristol isolate was used in this study. Lifespan assays were performed at 20 °C. Synchronous animal populations were generated by hypochlorite treatment of gravid adults to obtain tightly synchronized embryos that were allowed to develop into adulthood under appropriate, defined conditions. Spermidine (Sigma) was dissolved in sterilized water to a stock solution concentration of 100 mM. *Escherichia coli* (OP50) bacteria on seeded NGM plates were killed by UV irradiation for 10 min (0.5 J) using a UV crosslinker (BIO-LINK – BLX-E365, Vilber Lourmat). A range of spermidine concentrations was prepared by dilutions in 100 µl sterilized water and applied to the top of the agar medium (7 ml NGM plates). Plates were then gently swirled to allow drug to spread to the entire NGM surface. Identical solutions of drug-free water were used for the control plates. Plates were then allowed to dry overnight. The procedure was repeated each time worms were transferred to fresh plates (every 2–4 days during the first two weeks and every week thereafter).

For RNAi lifespan experiments worms were placed on NGM plates containing 0.5–1 mM IPTG and seeded with HT115(DE3) bacteria transformed with either the pL4440 vector or the test RNAi plasmid. Construction of the plasmid that directs the synthesis of a dsRNA corresponding to the *bec-1* gene in *E. coli* bacteria, which were subsequently fed to animals, as described previously^{40,59}. Progeny were grown at 20 °C through the L4 larval stage and then transferred to fresh plates, at groups of 10 worms per plate. The day of egg harvest and initiation of RNAi was used as *t* = 0. Animals were transferred to fresh plates every 2–4 days thereafter and were examined every day for touch-provoked movement and pharyngeal pumping, until death. Worms that died due to internally hatched eggs, an extruded gonad or desiccation due to crawling on the edge of the plates, were censored. Each survival assay was repeated three times and figures represent typical assays. Survival curves were created using the product-limit method of Kaplan and Meier. The log-rank (Mantel-Cox) test was used to evaluate differences between survivals and determine *P* values. We used the Prism software package (GraphPad Software) to carry out statistical analysis and to determine lifespan values.

***C. elegans* autophagy measurements.** To enable autophagy monitoring, we used a full-length DsRED::LGG-1 fusion. LGG-1 is the nematode orthologue of yeast Atg8/Aut7p and mammalian MAP-LC3, a protein involved in autophagosome formation. Construction of the p_{gcr-1}DsRED::LGG-1 reporter has previously been described⁵⁹. Transgenic embryos expressing DsRED were photographed on an Axioskop 2 Plus, epifluorescence microscope (Carl Zeiss). Images were acquired using a 540 ± 15 nm band-pass excitation filter and a 575 nm long-pass emission filter. Experiments were performed at 20 °C, with photography exposure time kept identical for each

embryo. Emission intensity was measured on grayscale images with a pixel depth of 8 bit (256 shades of grey). We calculated the mean and maximum pixel intensity for each embryo in these images using the ImageJ software (<http://rsb.info.nih.gov/ij/>). For each transgenic line, we processed at least 15 images over at least 3 independent trials. Statistical analyses were carried out using the Microsoft Office 2003 Excel software package (Microsoft Corporation). Mean values were compared using unpaired *t*-tests. For multiple comparisons, we used the one-factor (ANOVA) variance analysis corrected by the post hoc Bonferroni test.

Extraction of polyamines for LC/MS/MS measurements. For acid extraction of polyamines from yeast cells⁴⁸, culture equivalents of absorbance 20 were washed three times with double-distilled water, resuspended in 400 μ l ice-cold 5% TCA and incubated on ice for 1 h with vortexing every 15 min. Supernatants were neutralized with 100 μ l of 2 M K_2HPO_4 and stored at -80°C upon polyamine measurements using LC/MS/MS.

Extraction of polyamines from mice liver tissue and from flies was performed according to the freeze/thaw method described previously⁶⁰ with slight modifications. Briefly, about 50–75 mg of mouse liver tissue or 15–20 mg of whole flies were semi-homogenized using Fisherbrand Disposable Pestle System (Fisher Scientific) and polyamines extracted with 400 μ l 5% TCA by three repeated freeze-thaw cycles. After extraction, ammonium formate (0.4 M final concentration) was added to supernatants and stored at -80°C until polyamine measurements were performed using LC/MS/MS.

Polyamine measurements using LC/MS/MS. Polyamines were determined according to the method described previously⁶¹. All experiments were carried out on an Ultimate 3,000 System (Dionex, LC-Packings) coupled to a Quantum TSO Ultra AM (ThermoFinnigan) using an APCI ion source. The system was controlled by Xcalibur Software 1.4. The stationary phase was a Sequant ZIC-HILIC column (150 \times 2.1 mm, 3 μ m, 100 \AA). The elution solvent A was 50 mM ammonium formate in ultra pure water and solvent B was acetonitrile. Separation was performed with 15% acetonitrile for 2 min. Thereafter, the acetonitrile content was linearly decreased to 5% over 2 min. After 1 min, acetonitrile content was increased to 15% for column equilibration. Flow rate was set to 300 μ l min^{-1} .

Polyamines were detected in MRM mode using following transitions: spermidine (m/z 146 \rightarrow 72, CE 34 eV), putrescine (m/z 89 \rightarrow 72, CE 28 eV), bis(hexamethylene)-tri-amine as internal standard (m/z 216 \rightarrow 100, CE 36 eV). Calibration standards were prepared by spiking extraction buffer with specific concentrations of spermidine, putrescine and internal standard. 20 μ l of each sample were injected.

Electron microscopy of yeast cells. Yeast cells were aged to day 20 or logarithmically grown (day 0), transformed into spheroblasts and fixed in 2% glutaraldehyde (Sigma) for 1 hour. Spheroblastation was performed using zymolyase (20 U ml^{-1}), lyticase (100 U ml^{-1}) and glucuronidase/arylsulphatase (7 μ l ml^{-1}) (Roche) in 20 mM potassium phosphate buffer (pH 7.4) with 1.2 M sorbitol for 70 min at 28°C . Glutaraldehyde fixation was performed in 20 mM potassium phosphate buffer (pH 7.4) with addition of 0.4 M potassium chloride for osmotic stabilization of spheroblasts. Fixed cells were postfixated in osmium tetroxide and prepared for electron microscopy as described previously⁶². Thin sections were cut on a Reichert Ultracut microtome (Reichert-Jung Optische Werke) using a diamond knife (Diatome). The sections were collected on parlodion coated copper grids and stained with 6% uranyl acetate for 1 h followed by 2% lead citrate for 2 min. Electron micrographs were recorded with a Hitachi H-7,000 transmission electron microscope (Hitachi) operated at an acceleration voltage of 100 kV.

Spontaneous mutation frequency and budding index. Spontaneous mutation frequency was determined based on the appearance of mutants able to form colonies on agar plates containing 60 mg l^{-1} L-canavanine sulphate according to a published method¹. Mutation rates were calculated per 10^6 living (colony forming on YEPD) cells. Budding index was assessed by counting the percentage of budded cells after 10 s of sonication on ice using Sonifier 250 from Benson (duty cycle: 35; output control: 2.5) in micrographs of no more than 40 cells. For each sample, at least 500 cells were evaluated.

Immunoblotting, quantification of histone acetylation. Trichloroacetic acid yeast cell extracts were prepared according to a method described previously³⁴ using absorbances of 20–40 equivalents (depending on the age of culture) finally diluted in

350 μ l of 1 \times Laemmli. Hydrochloric acid extracts from mouse hepatocytes or human PBMC were obtained following the protocol described previously for HeLa cells⁵⁴.

Proteins were separated on 15% SDS-PAGE for immunoblot analysis on PVDF membrane (Millipore) using CAPS buffer (10 mM 3-(cyclohexylamino)-1-propanesulphonic acid, pH 11, 10% methanol) for transfer of proteins. Blots were probed with a total histone H3 recognizing rabbit polyclonal antibody (ab1791, Abcam) (1:5,000), which served as a loading control, as well as the following histone H3 modification antibodies (Upstate Biotechnology, Millipore): K9Ac (1:5,000), K14ac (1:5,000), K9+14Ac (1:10,000) and K18ac (1:10,000) according to the procedure suggested by the manufacturer. Peroxidase-conjugated affinity-purified secondary antibody was obtained from Sigma (A0545; 1:10,000).

Immunoblots were scanned using a densitometer (Molecular Dynamics, Model P.D. 300) and quantified with ImageQuant Version 5.1 (Molecular Dynamics). Importantly, protein extracts were initially applied to immunoblot analysis in nine different dilutions (serial steps of 1.3) to determine the range of protein loading that gave a linear response upon densitometry of the signals (for representative examples see Supplementary Information, Fig. S4). On the basis of these results, samples were subsequently used within this linear range. Similarly, film exposure times were adjusted to yield intensities that were previously confirmed to be in the linear range of quantification.

Samples that were directly compared to each other were always analysed on the same blot. For calculation of acetylation levels, intensities of acetylation specific blots were directly compared to respective intensities of blots probed with total histone H3 antibody to obtain the acetylation rate for each sample. Subsequently, acetylation rates of control samples were normalized to 1 and the relative acetylation of each sample was calculated accordingly.

Yeast nuclear extract preparation and HAT activity assay. Yeast nuclei were isolated from 200 ml BY4741 wild-type culture (grown for 24 h in SCD to stationary phase) as described previously⁵⁰. Nuclear extract was prepared using nuclear extraction buffer from BioVision's nuclear/cytosol fractionation kit (Bio Vision, K266-25) without dithiothreitol addition, according to the manufacturer's protocol. Incubation time was doubled to 80 min with vortexing every 8 min. Protein concentration was determined through Bradford, giving yields of approximately 1 mg ml^{-1} protein. Yeast nuclear extract was immediately subjected to HAT activity assays. For HAT-activity determination the commercially available HAT Activity Colorimetric Assay KIT from BioVision (Bio Vision K332-100) was used. HAT assays were performed according to the manufacturer's protocol. In brief, assays were performed with each 15 μ g of yeast nuclear extract or nuclear extract of HeLa-cells (Bio Vision K332-100-4), respectively. Spermidine was added at a final concentration of 100 mM 15 min after assay initiation. Development of tetrazolium dye was measured by absorption at 440 nm using a GeniosPro plate reader (Tecan). Background readings were done with samples without NADH generating enzyme, giving the nuclear extracts unspecific background activity and eliminate any possible negative effects of spermidine addition on the assay itself. For calculation of relative HAT activity linear regression over 100 min within the suggested assay time (95–195 min) was performed to determine the slope of dye development. Regression coefficients of $R^2 > 0.99$ were obtained. Calculated slopes of spermidine treated samples were compared to slopes of untreated samples which were set to a relative activity of 100%.

Yeast RNA isolation and affymetrix array analyses. Total RNA extraction from chronologically aged yeast cells (with or without spermidine application) by glass bead disruption were performed using RNeasy MiniKit (Quiagen) according to the manufacturer's instructions. Cells (10^8) were used after shock-freezing in liquid nitrogen and storage at -80°C on preparation. RNA of two independent ageing experiments at days 3 and 10 (biological replicates) were applied to Affymetrix array analyses.

Syntheses of cDNA and hybridisation experiments were outsourced to the Microarray Facility Tuebingen, Germany, an authorized Affymetrix Service Provider. Hybridization was performed on high-density oligonucleotide arrays Yeast Genome 2.0 (Affymetrix). Both, experimental and data analysis workflow were fully compliant with the MIAME 2.0 Standard. Annotation Data for the Yeast Genome 2.0 Array were supplied by Affymetrix. Raw data were normalized with GCRMA⁶³ using CarmaWeb⁶⁴. *P* values were calculated with a paired *t*-test comparing untreated (controls) with treated (spermidine supplemented) samples at the respective time-points using TM4 MeV software⁶⁵.

Quantitative reverse transcription real-time PCR (q-RT-PCR). q-RT-PCR analysis of total RNA was performed in a RotorGene 6,000 (Corbett Life Science) using the SensiMix One-step kit from Quantace. Primers (listed in Supplementary Information, Table S5) were designed using the online available software Primer3 (<http://frodo.wi.mit.edu/primer3/>)⁶⁶. Total RNA was isolated as described above (see section on Yeast RNA Isolation). To remove traces of DNA, a DNaseI digest was performed by incubating 1 µg of RNA for 30 min at 37 °C with 1 U DNaseI (Fermentas) in the appropriate buffer with MgCl₂. The reaction was stopped by addition of EDTA to a final concentration of 2.5 mM and incubation at 65 °C for 10 min. The q-RT-PCR reaction was performed in a total volume of 10 µl containing 4 ng of DNaseI treated RNA according to the manufacturer's protocol.

Relative mRNA concentrations of spermidine treated samples normalized to controls were determined using the 2^{-ΔC_T} method as described elsewhere⁶⁷. In short, the C_T values of spermidine-treated samples were subtracted from that of control samples, resulting in -ΔC_T. Relative concentrations were calculated as 2^{-ΔC_T}.

Chromatin immunoprecipitation assay (ChIP) and quantitative real-time PCR (qPCR). ChIP assays were performed according to the online available protocol of the Haber Lab (<http://www.bio.brandeis.edu/haberlab/jehsite/pdfs/chipmeth.pdf>) that is based on the previous publications^{68,69}. Briefly, spermidine-treated and untreated cells (2 × 10⁸ cells in total) were collected at day 7 of a chronological ageing experiment, washed once with TBS and lysed in the presence of glass beads on a multitube vortexer for 45 min at 4 °C. Notably, chromatin was not crosslinked during our procedure. Subsequent sonication of the lysate (9 cycles with 10 s for each cycle) was performed on ice with Sonifier 250 from Benson. For immunoprecipitation, 70 µl of the lysate (representing ~3 × 10⁷ cells) was diluted 1:5 in lysis buffer containing the histone H3-K18Ac antibody (Upstate Biotechnology, Millipore; final concentration 1:300) to a final volume of 350 µl and incubated overnight (16 h) at 4 °C (IP sample). A second aliquot of the lysate was incubated on ice in parallel giving the Non-IP sample. Precipitation of IP samples was performed with the PureProteome Protein G Magnetic Bead System (Millipore) for 15 min at room temperature using 30 µl of bead suspensions according to the manufacturer's instructions. After several washing steps and final elution, samples were treated with proteinase K (0.2 mg ml⁻¹) for 4 h at 37 °C. DNA was extracted with phenol and precipitated using LiCl and ethanol and finally dissolved in 50 µl TE buffer.

qPCR of ChIP assay samples was performed in a RotorGene 6,000 (Corbett Life Science) using the DyNAmo Flash SYBR Green qPCR Kit (Finnzymes). Primers specific for the indicated promoter regions (listed in Supplementary Information, Table S5) were designed using the online available software Primer3 (<http://frodo.wi.mit.edu/primer3/>)⁶⁶. The qPCR reaction was performed in a total volume of 20 µl according to the manufacturer's protocol. Relative concentration of precipitated DNA (and therefore relative promoter acetylation) was calculated for each indicated promoter region by, first, normalizing the qPCR signals of IP samples to the respective Non-IP samples (in order to correct for unspecific differences before chromatin precipitation) and, second, normalising to the respective signal obtained for the *ATG7* promoter region. Data are presented as means of qPCR duplicates of three independent ChIP samples (each from independent biological samples).

Statistical analyses. For *Drosophila* experiments, log rank and Wilcoxon, as well as a Kruskal-Wallis test, was used (for details see section on *Drosophila* lifespan experiments). Statistical analysis of Affimetrix array data was performed using

the TM4 MeV software (for details see Supplementary Information). Statistical analyses of yeast experiments were performed using unpaired *t*-test for single comparisons and a one-factor analysis of variance (ANOVA) corrected by the post hoc Bonferroni test for multiple comparisons. Except for replicative ageing (see section on replicative life span of yeast), yeast ageing experiments were analysed by a two-factor ANOVA with time and strain/condition as independent factors corrected by the post-hoc Bonferroni test.

48. Balasundaram, D., Tabor, C. W. & Tabor, H. Spermidine or spermine is essential for the aerobic growth of *Saccharomyces cerevisiae*. *Proc. Natl Acad. Sci. USA* **88**, 5872–5876 (1991).
49. Gueldener, U., Heinisch, J., Koehler, G. J., Voss, D. & Hegemann, J. H. A second set of loxP marker cassettes for Cre-mediated multiple gene knockouts in budding yeast. *Nucleic Acids Res.* **30**, e23 (2002).
50. Buttner, S. *et al.* Endonuclease G regulates budding yeast life and death. *Mol. Cell* **25**, 233–246 (2007).
51. Lotze, M. T. & Tracey, K. J. High-mobility group Box 1 protein (HMGB1): nuclear weapon in the immune arsenal. *Nature Rev. Immunol.* **5**, 331–342 (2005).
52. Kirisako, T. *et al.* Formation process of autophagosome is traced with Apg8/Aut7p in yeast. *J. Cell Biol.* **147**, 435–446 (1999).
53. Noda, T., Matsuura, A., Wada, Y. & Ohsumi, Y. Novel system for monitoring autophagy in the yeast *Saccharomyces cerevisiae*. *Biochem. Biophys. Res. Commun.* **210**, 126–132 (1995).
54. Vermes, I., Haanen, C., Steffens-Nakken, H. & Reutelingsperger, C. A novel assay for apoptosis. Flow cytometric detection of phosphatidylserine expression on early apoptotic cells using fluorescein labelled annexin V. *J. Immunol. Methods* **184**, 39–51 (1995).
55. Criollo, A. *et al.* Regulation of autophagy by the inositol trisphosphate receptor. *Cell Death Differ.* **14**, 1029–1039 (2007).
56. Ellman, G. L. Tissue sulfhydryl groups. *Arch. Biochem. Biophys.* **82**, 70–77 (1959).
57. Riener, C. K., Kada, G. & Gruber, H. J. Quick measurement of protein sulfhydryls with Ellman's reagent and with 4, 4'-dithiodipyridine. *Anal. Bioanal. Chem.* **373**, 266–276 (2002).
58. Brenner, S. The genetics of *Caenorhabditis elegans*. *Genetics* **77**, 71–94 (1974).
59. Samara, C., Syntichaki, P. & Tavernarakis, N. Autophagy is required for necrotic cell death in *Caenorhabditis elegans*. *Cell Death Differ.* **15**, 105–112 (2008).
60. Minocha, R., Shortle, W. C., Long, S. L. & Minocha, S. C. A rapid and reliable procedure for extraction of cellular polyamines and inorganic ions from plant tissues. *J. Plant Growth Regul.* **13**, 187–193 (1994).
61. Gianotti, V. *et al.* A new hydrophilic interaction liquid chromatography tandem mass spectrometry method for the simultaneous determination of seven biogenic amines in cheese. *J. Chromatogr. A* **1185**, 296–300 (2008).
62. Fahrenkrog, B., Hurt, E. C., Aebi, U. & Pante, N. Molecular architecture of the yeast nuclear pore complex: localization of Nsp1p subcomplexes. *J. Cell Biol.* **143**, 577–588 (1998).
63. Wu, Z., Irizarry, R. A., Gentleman, R., Martinez-Murillo, F. & Spencer, F. A model-based background adjustment for oligonucleotide expression arrays. *J. Am. Stat. Assoc.* **99**, 909–918 (2004).
64. Rainer, J., Sanchez-Cabo, F., Stocker, G., Sturn, A. & Trajanoski, Z. CARMAweb: comprehensive R- and bioconductor-based web service for microarray data analysis. *Nucleic Acids Res.* **34**, W498–W503 (2006).
65. Saeed, A. I. *et al.* TM4: a free, open-source system for microarray data management and analysis. *Biotechniques* **34**, 374–378 (2003).
66. Rozen, S. & Skaletsky, H. Primer3 on the WWW for general users and for biologist programmers. *Methods Mol. Biol.* **132**, 365–386 (2000).
67. Livak, K. J. & Schmittgen, T. D. Analysis of relative gene expression data using real-time quantitative PCR and the 2^{-ΔΔC_T} method. *Methods* **25**, 402–408 (2001).
68. Strahl-Bolsinger, S., Hecht, A., Luo, K. & Grunstein, M. SIR2 and SIR4 interactions differ in core and extended telomeric heterochromatin in yeast. *Genes Dev.* **11**, 83–93 (1997).
69. Evans, E., Sugawara, N., Haber, J. E. & Alani, E. The *Saccharomyces cerevisiae* Msh2 mismatch repair protein localizes to recombination intermediates *in vivo*. *Mol. Cell* **5**, 789–799 (2000).

DOI: 10.1038/ncb1975

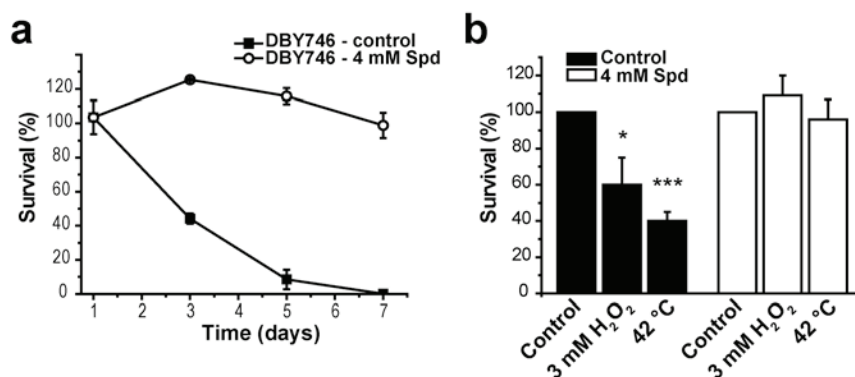


Figure S1 Spermidine treatment of yeast results in strong resistance against heat shock and hydrogen peroxide treatment. **(a)** Survival determined by clonogenicity during chronological ageing of wild type yeast (DBY746) with (○) and without (■) addition of 4 mM spermidine at day 1. Data represent means ± SEM (n = 4). **(b)** Survival of

pre-aged wild type cells stressed for 4 h with hydrogen peroxide (3 mM H₂O₂) or heat shock (42 °C) compared to unstressed cells. Cells were chronologically aged until day 24 with or without addition of 4 mM spermidine. Data represent means ± SEM (n = 4). *p < 0.05 and ***p < 0.001

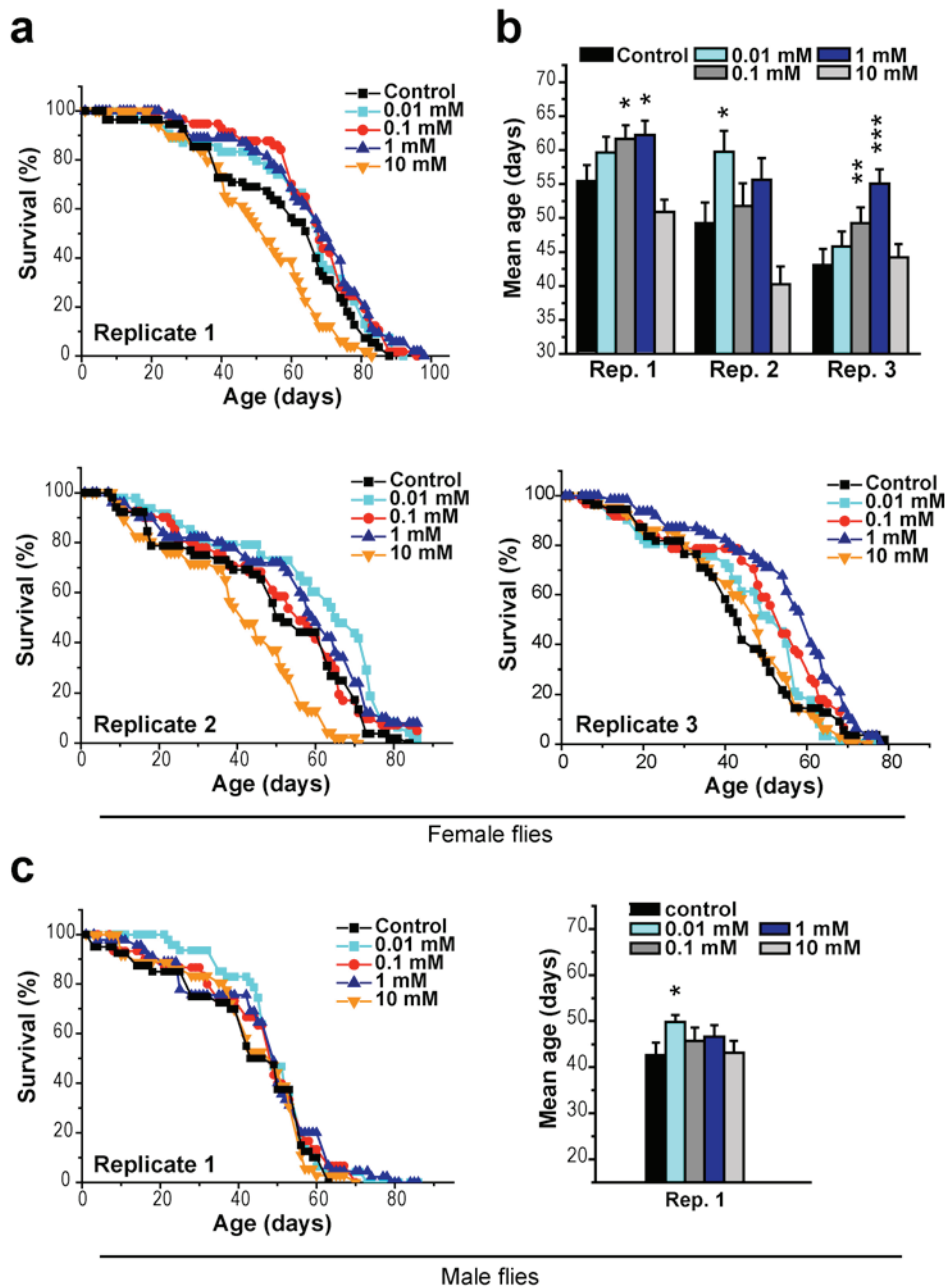


Figure S2 Administration of spermidine extends the life span of *Drosophila melanogaster*. **(a)** Replicates of female *Drosophila melanogaster* ageing experiments with and without (■) supplementation of normal food with various concentrations of spermidine. **(b)** Mean life spans calculated from the experiments shown in (a). Data represent means

± SEM of 40-60 flies. **p* < 0.05, ***p* < 0.01 and ****p* < 0.001. **(c)** *Drosophila melanogaster* ageing experiment of males with and without (■) supplementation of normal food with various concentrations of spermidine and respective mean life spans. Data represent means ± SEM of 40-60 flies. **p* < 0.05.

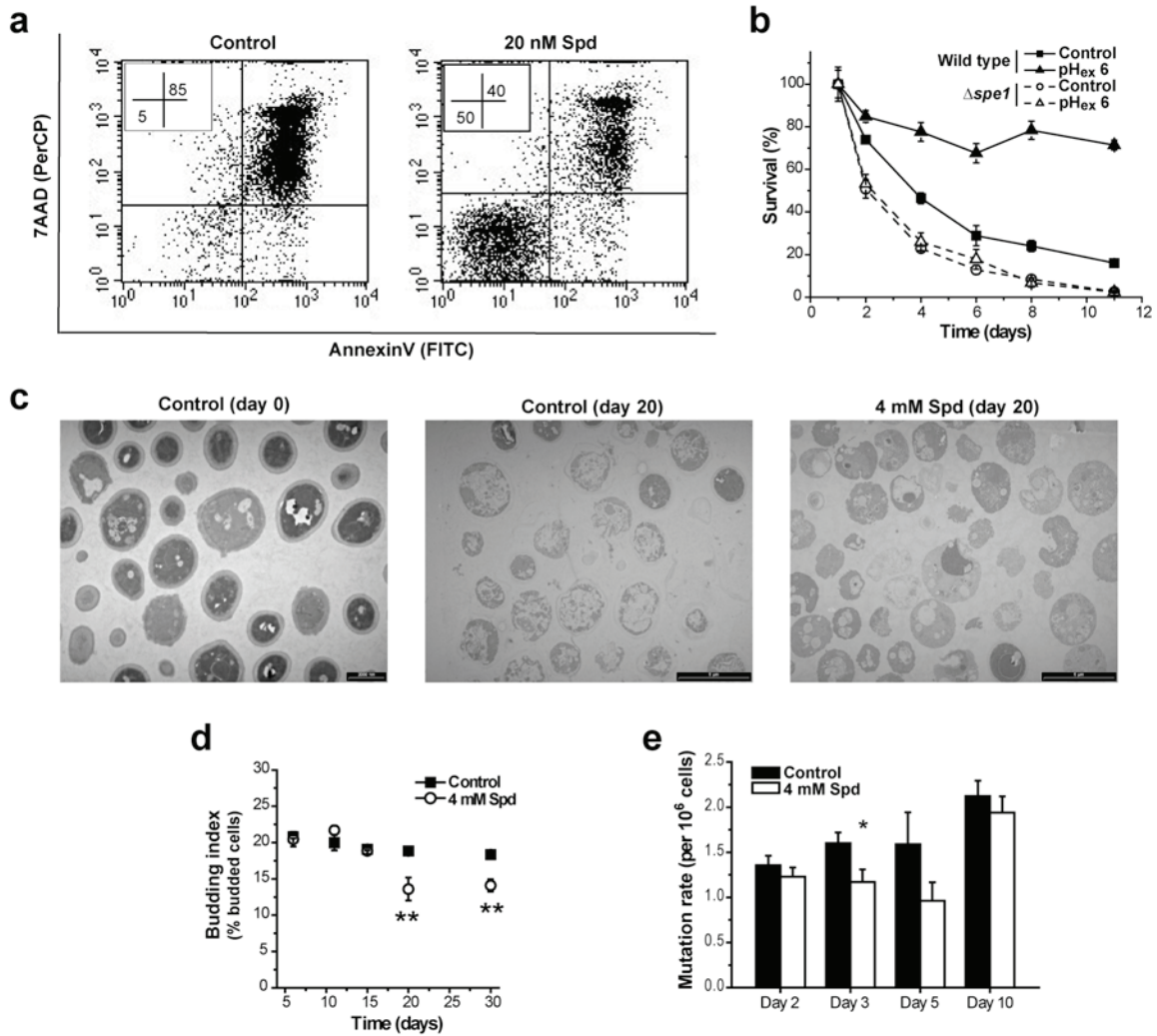


Figure S3 Spermidine inhibits necrotic cell death of ageing yeast and human PBMC. **(a)** Quantification (FACS analysis) of phosphatidylserine externalisation (FITC channel) and loss of membrane integrity indicative of necrosis (PerCP channel) using AnnexinV/7-ADD costaining of 12 days old human PBMC. Unstained cells were considered as viable. Dot plots with 30,000 cells evaluated of a representative experiment are shown. Numbers indicate the percentage of cells located in their respective gate. **(b)** Chronological ageing of wild type (closed symbols) and $\Delta spe1$ (open symbols) with ($\blacktriangle, \triangle$) and without (\blacksquare, \square) adjustment of extracellular pH to 6 (± 0.5). Data represent means \pm SEM (n = 3). **(c)** Overview pictures of

electron microscopy of 20 days old wild type yeast cells aged with or without (control) treatment of 4 mM spermidine and of healthy young cells. Higher resolution images of representative cells are shown in Figure 3E. **(d)** Budding index of wild type cells at indicated time points during chronological ageing with (o) or without (\bullet) application of 4 mM spermidine. Data represent means \pm SEM (n = 3) with at least 500-1000 cells evaluated for each replicate. $**p < 0.01$. **(e)** Mutation rate per 10⁶ living cells determined by canavanine resistance of wild type cells at indicated time points during chronological ageing with (open bars) or without (closed bars) application of 4 mM spermidine. Data represent means \pm SEM (n = 5). $*p < 0.05$

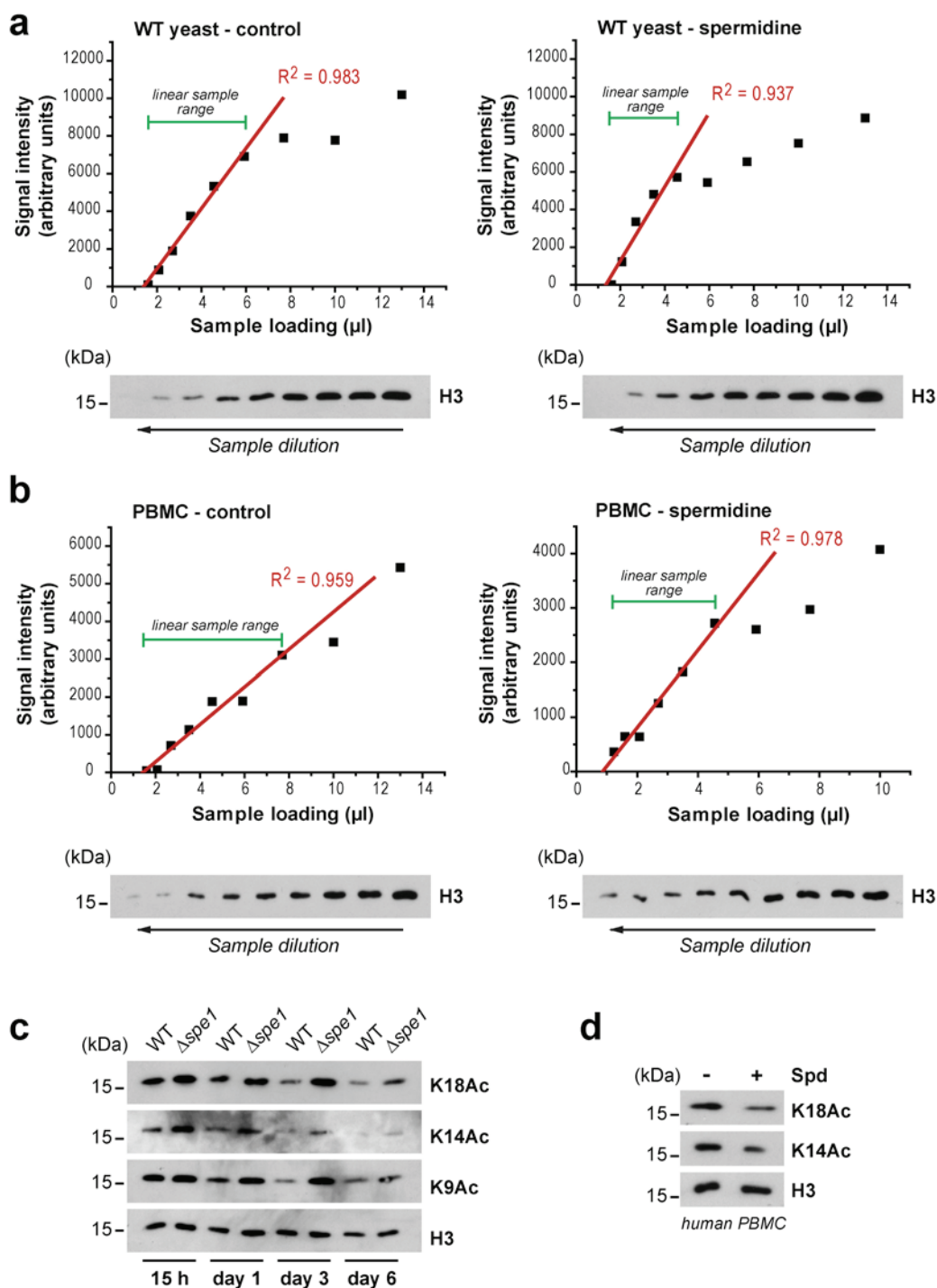


Figure S4 Serial dilutions were initially applied to immunoblot analysis in order to determine the linear range of sample loading and quantification by densitometry. **(a, b)** Representative examples of the identification of the linear range for quantitative immunoblot analyses are presented. Linear regression was performed after densitometry of shown immunoblot analyses from yeast **(a)** and PBMC **(b)** protein extracts aged with or without (control) application of spermidine for 16 days **(a)** or 6 days **(b)** in order to determine the linear range of sample loading and quantification. Blots were probed with an antibody specific for total histone H3. Subsequently, samples were

applied to immunoblot analysis exclusively within this linear range for the quantification of spermidine effects on histone acetylation using acetylated lysine specific antibodies (see Methods for details). **(c)** Representative immunoblot analysis of wild type and Δspe1 yeast cell extracts 15 hours past inoculation and after 1, 3 and 6 days of chronological ageing. Blots were probed with antibodies against total histone H3 or H3 acetylation sites at the indicated lysine residues. **(d)** Immunoblot analysis of human PBMC extracts after 6 days of ageing in the presence (+) or absence (-) of 20 nM spermidine. A representative blot is shown.

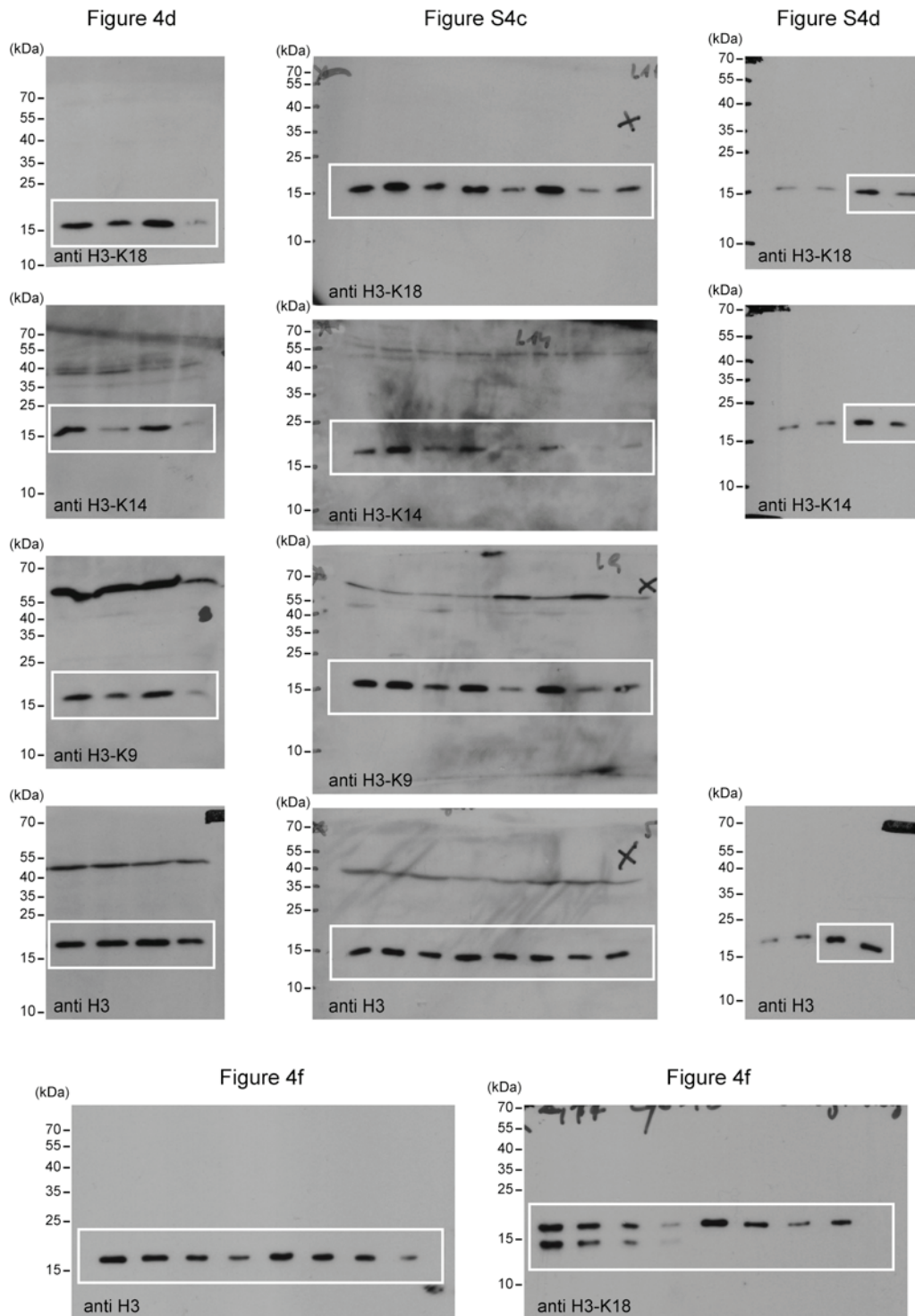


Figure S5 Full scans of key western blots presented in this study. Rectangles delimit cropped areas used in the indicated figures.

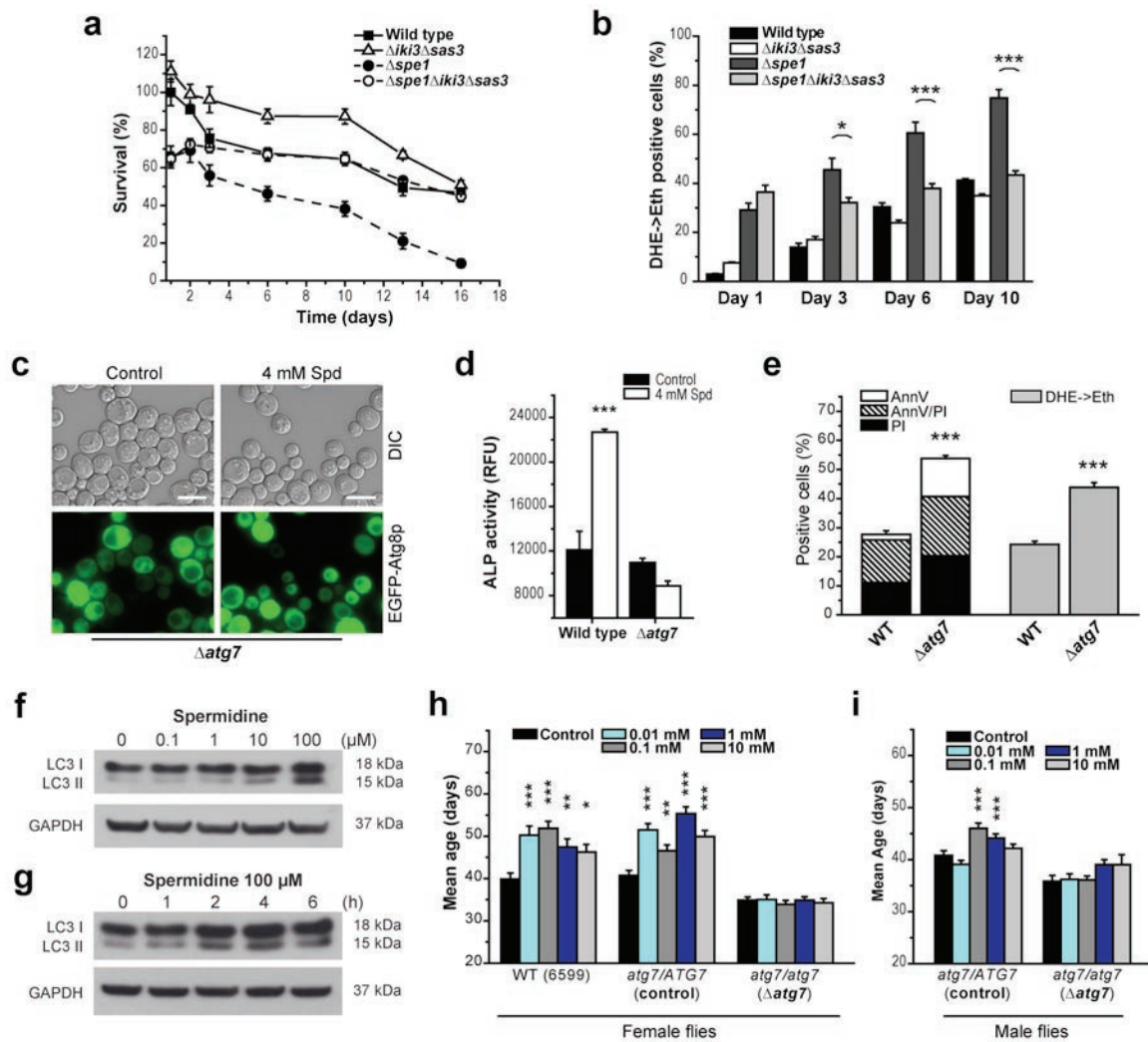


Figure S6 *ATG7*-dependent autophagy protects against age-induced programmed death and is critical for spermidine-mediated life span extension. **(a)** Chronological ageing of wild type (●), $\Delta iki3\Delta sas3$ (▲), $\Delta spe1$ (●) and $\Delta spe1\Delta iki3\Delta sas3$ (○) cells. Data represent means \pm SEM

($n = 4$). **(b)** Quantification (FACS analysis) of ROS accumulation using DHE staining of cells obtained from the chronological ageing experiment shown in (a). Data represent means \pm SEM ($n = 4$). * $p < 0.05$, *** $p < 0.001$

Supplementary Table S1

Modulation of yeast chronological ageing upon single disruption of genes involved in histone acetylation and deacetylation.

The effects on chronological ageing observed in 28 single deletion strains of genes involved in histone acetylation (***bold italic*** characters) or deacetylation (*italic* characters) are presented. All strains were aged with and without application of 4 mM spermidine and survival was determined by clonogenicity. Deletion strains were assigned to one of six categories, depending on the effects on survival during ageing and the ability of spermidine to improve this survival.

Survival during chronological ageing (compared to WT)	Pro-survival effect of spermidine application (compared to WT)	Single deletion of
increased during early ageing (day 5 to 15)	reduced	<i>SAS3, IKI3, ELP3</i> ¹
strongly reduced	increased during early ageing (due to fast death of control cultures), BUT diminished or absent at later time points (day 15 to 25)	<i>GCN5, SGF73, HDA2</i>
not affected	slightly reduced during early ageing (day 5 to 15)	<i>AHC1</i>
slightly increased	not affected	<i>HDA1</i>
slightly reduced	not affected	<i>SPT10, RXT2, SDS3, SAP30</i>
not affected	not affected	<i>HAT1, HPA2, HPA3, YNG1, HDA3, HOS1, HOS2, HOS3, HOS4, RPD3, PHO23, SIR2, HST1, HST2, SET3, SIF2</i>

¹The pro-survival effect of spermidine in the ***ELP3*** deleted strain was only reduced until day 10 of ageing. ***Bold italic*** characters indicate genes involved in the process of histone acetylation, while *italic* characters indicate genes involved in deacetylation.

Supplementary Table S2

Spermidine treatment induces the expression of autophagy-related genes during yeast ageing.

A subset of 50 genes related to macroautophagy, microautophagy or autophagy in general (all genes listed in GO:0016236, GO:0016237 and GO:0006914 obtained from SGD on June, 1st 2008) have been analysed (based on Affymetrix array data) for differential expression during chronological ageing of yeast upon treatment with 4 mM spermidine.

Day 3			Differential expression by spermidine			Day 10		
Gene	Factor	P-value	Gene	Factor	P-value			
<i>ATG10</i>	1.39	0.012	<i>ATG10</i>	0.94	0.453			
<i>ATG12</i>	1.34	0.348	<i>ATG12</i>	1.23	0.134			
<i>ATG13</i>	1.33	0.044	<i>ATG13</i>	1.25	0.327			
<i>ATG14</i>	2.01	0.032	<i>ATG14</i>	1.42	0.048			
<i>ATG16</i>	2.03	0.194	<i>ATG16</i>	1.74	0.240			
<i>ATG18</i>	1.30	0.194	<i>ATG18</i>	1.76	0.030			
<i>ATG20</i>	1.22	0.684	<i>ATG20</i>	1.43	0.091			
<i>ATG21</i>	1.56	0.290	<i>ATG21</i>	1.74	0.057			
<i>ATG29</i>	1.86	0.316	<i>ATG29</i>	2.13	0.064			
<i>ATG5</i>	1.20	0.012	<i>ATG5</i>	1.43	0.018			
<i>ATG7</i>	1.64	0.144	<i>ATG7</i>	2.22	0.039			
<i>PTC6</i>	1.02	0.402	<i>PTC6</i>	1.02	0.925			
<i>VPS15</i>	1.48	0.241	<i>VPS15</i>	1.93	0.137			
<i>VPS30</i>	1.73	0.422	<i>VPS30</i>	1.73	0.015			
<i>VPS34</i>	1.03	0.869	<i>VPS34</i>	1.11	0.004			
<i>CMD1</i>	1.11	0.316	<i>CMD1</i>	1.00	0.723			
<i>GTR2</i>	0.89	0.200	<i>GTR2</i>	0.48	0.192			
<i>MEH1</i>	1.08	0.541	<i>MEH1</i>	1.39	0.169			
<i>NVJ1</i>	1.41	0.388	<i>NVJ1</i>	1.69	0.159			
<i>PEP4</i>	0.84	0.394	<i>PEP4</i>	1.11	0.416			
<i>SLM4</i>	1.10	0.224	<i>SLM4</i>	2.08	0.064			
<i>VAC8</i>	1.03	0.852	<i>VAC8</i>	1.12	0.648			
<i>VTC1</i>	1.28	0.468	<i>VTC1</i>	1.33	0.125			
<i>VTC2</i>	0.97	0.768	<i>VTC2</i>	0.73	0.235			
<i>VTC3</i>	1.09	0.783	<i>VTC3</i>	0.90	0.656			
<i>VTC4</i>	1.45	0.440	<i>VTC4</i>	0.84	0.460			

macroautophagy

microautophagy

Table continues on next page...

Table continued from previous page.

Gene	Factor	P-value	Gene	Factor	P-value
<i>ATG1</i>	1.42	0.071	<i>ATG1</i>	1.12	0.089
<i>ATG11</i>	1.23	0.053	<i>ATG11</i>	1.67	0.163
<i>ATG15</i>	1.27	0.121	<i>ATG15</i>	1.20	0.035
<i>ATG17</i>	1.17	0.542	<i>ATG17</i>	1.32	0.267
<i>ATG19</i>	1.83	0.133	<i>ATG19</i>	3.12	0.128
<i>ATG2</i>	1.14	0.258	<i>ATG2</i>	1.48	0.141
<i>ATG22</i>	1.21	0.234	<i>ATG22</i>	1.10	0.622
<i>ATG23</i>	1.39	0.094	<i>ATG23</i>	1.09	0.223
<i>ATG26</i>	1.22	0.403	<i>ATG26</i>	1.26	0.040
<i>ATG27</i>	1.15	0.183	<i>ATG27</i>	1.13	0.257
<i>ATG3</i>	1.08	0.370	<i>ATG3</i>	1.55	0.097
<i>ATG4</i>	1.24	0.571	<i>ATG4</i>	1.07	0.365
<i>ATG8</i>	1.30	0.185	<i>ATG8</i>	0.97	0.436
<i>ATG9</i>	1.40	0.168	<i>ATG9</i>	1.87	0.177
<i>CCZI</i>	1.54	0.150	<i>CCZI</i>	1.06	0.495
<i>CIS1</i>	1.57	0.199	<i>CIS1</i>	1.50	0.275
<i>GSG1</i>	0.99	0.588	<i>GSG1</i>	0.87	0.527
<i>SEC23</i>	0.94	0.499	<i>SEC23</i>	1.25	0.289
<i>IRS4</i>	1.10	0.278	<i>IRS4</i>	0.76	0.085
<i>MON1</i>	1.49	0.516	<i>MON1</i>	1.09	0.417
<i>SEC16</i>	1.21	0.738	<i>SEC16</i>	0.86	0.155
<i>SEC24</i>	1.18	0.136	<i>SEC24</i>	0.95	0.359
<i>TAX4</i>	1.14	0.449	<i>TAX4</i>	1.09	0.401
<i>VAM3</i>	1.01	0.720	<i>VAM3</i>	0.94	0.383

microautophagy

Supplementary Table S3

Spermidine extends the life span of nematodes in a Beclin 1 dependent fashion.

C. elegans mean and maximum life spans are shown from N2 wild type and *bec-1* RNAi knockdown animals aged with or without supplementation of normal food with 0.2 mM spermidine (Spd).

Strain	Mean life span ± SEM (days)	Max life span (days)	Deaths/total	<i>P</i> value
N2 (wild type)	22.1 ± 0.8	36	111/130	
N2 + 0.2 mM Spd	25.5 ± 1.3	41	110/130	< 0.0001 Compared to N2
<i>bec-1(RNAi)</i>	15.8 ± 1.5	26	110/130	
<i>bec-1(RNAi)</i> + 0.2 mM Spd	17.1 ± 1.6	29	109/130	< 0.0001 Compared to N2 + 0.2 mM Spd

Supplementary Table S4

Primers used for gene disruption and cloning.

Sequences of control primers kan-B, Leu-B (used for verification of *IKI3* and *SPE1* deletion) and Ura-C (used for verification of *SAS3* deletion) were according to Gueldener et al.(2).

Primer for...	Sequence
loxP- <i>Ura3</i> -loxP cassette (<i>SAS3</i> deletion using pUG72)	5'-TTCCTTCTTCATTAATTAGTCTCCGTATAAATTGCAGATACAGCTGAAGCTTCGTACGC-3' 5'-ACATGTATATGCTTATATCCAATATATACCCATCGCCGCGCATAGGCCACTA GTGGATCTG-3'
loxP- <i>Leu2</i> -loxP cassette (<i>SPE1</i> deletion using pUG73)	5'-GTTCTACAAC TTTTCATAGTAATCAAAACCTTTGAATTTCAAAC TACTCAGCTGAAGCTTCGTACGC-3' 5'-CACCCCCTCCGTCTCTCTTGCGAAAGTCGTGGTTAAATATATCCTGCATAGGC CACTAGTGGATC-3'
Deletion control primers (forward)	5'-AGGCCAATTGAACAAGAAAT-3' (<i>SAS3</i>) 5'-GTACTAGTAGAGTTCAAGACA-3' (<i>IKI3</i>) 5'-AATTTTAATCTGCGCCGTGC-3' (<i>SPE1</i>)
Deletion control primers (reverse)	5'-GGATGTATGGGCTAAATG-3' (kan-B) 5'-TTGGCTAATCATGACCCC-3' (Ura-C) 5'-AGTTATCCTTGGATTGG-3' (Leu-B)
pUG35-Ura/ <i>NHP6A</i>	5'-ATCTGAATTCATGGTCACCCCAAGAGAAC-3' 5'-ATCTGAATTCAGCCAAAGTGGCGTTATATAAC-3'
pUG36-Ura/ <i>ATG8</i>	5'-ATCTGAATTCATGAAGTCTACATTTAAGTCTGAATATCC-3' 5'-ATCTATCGATCTACCTGCCAAATGTATTTTCTCC -3'

Supplementary Table S5

Primers used for quantitative real time PCR (qPCR) and quantitative reverse transcription real time PCR (q-RT PCR).

Primer specific for...	Sequence
Gene (qRT-PCR)	
<i>ATG7</i> (forward)	5'-TTGCAATACGATGTTCTGACTTGA-3'
<i>ATG7</i> (reverse)	5'-TGCTAGCTTACCTTGACATTCCTT-3'
<i>ATG11</i> (forward)	5'-CACTGCACCTACCCAGCAAGAA-3'
<i>ATG11</i> (reverse)	5'-AGCAGCTGATCGGGAGGAATCT-3'
<i>ATG15</i> (forward)	5'-AGGAAGAACACGCCATGTGGATA-3'
<i>ATG15</i> (reverse)	5'-CAAAATCTTCCGGCTCTGTTCA-3'
Promotor (qPCR)	
<i>pATG7</i> (forward)	5'-CATGAGATTCCTTTGGACACCCTTT-3'
<i>pATG7</i> (reverse)	5'-TGCATAACTTAAGACCCTTTCTGACGA-3'
<i>pNMD3</i> (forward)	5'-TTGAAGCTCATCGCATTGGAAAAG-3'
<i>pNMD3</i> (reverse)	5'-TGAATTCATCCTTTTGTCAAATTCC-3'
<i>pDBP8</i> (forward)	5'-TTTTGCCATAGAAGCCGTGAGAAG-3'
<i>pDBP8</i> (reverse)	5'-GATGCTACGGAGATCTAAAGCGTC-3'
<i>pMTG2</i> (forward)	5'-TTCACCTCCCCGAAATAGTACTGAAGGA-3'
<i>pMTG2</i> (reverse)	5'-GCCGTAATTCTCTTTTGAAAACGCTAGA-3'
<i>pCDC23</i> (forward)	5'-GCGTACATAAAAAGCACTTCGGGTA-3'
<i>pCDC23</i> (reverse)	5'-TGTCGTCATTCATGGTTCTAAATGC-3'
<i>pPRP8</i> (forward)	5'-ATTTAAAGTGACCATGGCAGAAGGA-3'
<i>pPRP8</i> (reverse)	5'-GGCGGTAGTCCACTCATCTTTCTTT-3'
<i>pSOL3</i> (forward)	5'-AACGCCGAATTTACAACCTCGAAACT-3'
<i>pSOL3</i> (reverse)	5'-CCATTGTCGGGGATAAAAAGGTAAG-3'
<i>pTDA11</i> (forward)	5'-AGTGTAAGTATCACAAATCAAGCAAACAA-3'
<i>pTDA11</i> (reverse)	5'-ACCCTTCATCACCTTTGGAATCAC-3'

Supplementary Information

Supplementary Results and Discussion

Yeast Doubling Times and Depletion of Polyamines.

Polyamines are required for normal growth of yeast cells¹. Therefore, *spe1* mutant cells were grown to stationary phase in a way that they retained sufficient polyamine concentrations when growing, but displayed maximal diminution of intracellular polyamines upon entry into stationary phase, where chronological ageing begins. As a result, Δ *spe1* cells arrested growth at 30-40% lower cell density compared to wild type cells. This was achieved by growing Δ *spe1* cells (that were kept on YPD plates before) for approximately 13-14 generations (including overnight culture) in normal SCD.

Decreased doubling times of Δ *spe1* cells (80.9 ± 0.3 min) compared to wild type (91.7 ± 0.2 min) (likely due to the requirement of polyamines during aerobic growth¹) confirmed that the observed Δ *spe1* phenotypes were not due to an increased growth rate which could in principle cause accelerated ageing.

Cell death triggered by depletion of spermidine is necrotic, not apoptotic.

Depletion of polyamines (e.g. spermidine) by deletion of *SPE1*, coding for the enzyme that catalyses the rate limiting step of polyamine biosynthesis, precipitates premature ageing accompanied by markers of oxidative stress (see main text of the manuscript, Figure 2).

Enhanced generation of oxygen radicals upon *SPE2* deletion has also been observed in growing cells². Since oxidative stress can cause apoptosis in yeast^{3, 4} we determined apoptotic markers of wild type and polyamine depleted $\Delta spe1$ cells. Surprisingly, the frequency of apoptotic events (that is cells that exhibit DNA-fragmentation detectable by TUNEL or phosphatidylserine externalisation detectable with Annexin V) was not affected by *SPE1* deletion (Fig. 2e). Instead, we observed an increase in necrotic, PI positive cells in $\Delta spe1$ cultures compared to wild type controls (Fig. 2e). Accordingly, deletion of apoptotic effector molecules (including the yeast caspase, Yca1p⁵; apoptosis-inducing factor, Aif1p⁶; endonuclease G, Nuc1p⁷; or the serine protease HtrA2/OMI, Nma111p⁸) in the background of $\Delta spe1$ did not prevent the ageing-associated death that was accelerated by polyamine depletion (data not shown). Again, the necrotic phenotype of $\Delta spe1$ cells was completely abolished by application of 0.1 mM spermidine (Fig. 2d, e). We therefore conclude that depletion of intracellular polyamines can precipitate premature chronological ageing via non-apoptotic, presumably necrotic death of yeast cells.

Spermidine prolongs life span in various ageing models in a pH-independent fashion

Administration of spermidine to chronologically ageing yeast or alkalinisation of the medium with NaOH both prolonged yeast life span and increased the extracellular and cytosolic pH (data not shown). However, the life span-extending effect of alkalinisation is strictly dependent on intracellular polyamines, as it was only observed in wild type, not in $\Delta spe1$ cultures (Fig. S3b). It is important to note that in all other models used (including yeast replicative life span), the effect of spermidine was pH independent. In

fact, the pH was either titrated to control levels upon addition of spermidine to yeast media or to the drinking water of mice or simply did not change the pH of mammalian cell culture media, worm or fly media (which were all sufficiently buffered).

Recently, it has been reported that one of the major causes of yeast chronological ageing is the excessive production of acetic acid⁹. As none of the other ageing models used in this study were associated with such an (extreme) extracellular acidification, it seems to be a unique circumstance for the yeast system. Nevertheless, the ageing mechanisms identified by this system are transferable to higher eukaryotes including mammals¹⁰⁻¹².

Spermidine application counteracts age-induced necrotic cell death.

Upon spermidine application, chronological ageing yeast exhibited a drastic reduction in markers of necrosis and oxidative stress as compared to untreated controls (Fig. 3a-c). In contrast, externalisation of phosphatidylserine, an early apoptotic marker (Annexin V⁺ PI⁻ cells), remained largely unaltered. Instead, loss of membrane integrity due to primary necrosis (PI positivity) and late apoptosis resulting in secondary necrosis (Annexin V⁺ PI⁺) was reduced from 50% to less than 10% in spermidine-treated cultures as late as after 18 days of ageing (Fig. 3c). We conclude that death associated with chronological ageing of yeast is mainly mediated by spermidine-inhibitable necrosis-like cell death.

Inhibition of cell death rather than regrowth of death-resistant mutants mediate life span extension upon spermidine application.

To verify that the improved survival of spermidine-treated cultures is indeed due to cell death inhibition rather than regrowth of mutants¹³, we determined the budding index and

mutation frequency during the course of ageing (Fig. S3d). While application of spermidine did not affect the percentage of budded cells until day 15, it actually reduced the budding index by ~30% at later points in the experiment (Fig. S3d). This has also recently been connected to chronological life span extension¹⁴. The mutation frequency, which was monitored by assessing the appearance of canavanine resistant mutants¹³, was slightly reduced by spermidine (Fig. S3e), indicating that spermidine might actually increase genomic stability. Thus, these observations raise the possibility that epigenetic modifications rather than genetic changes are responsible for the positive effects of spermidine on longevity.

Inhibition of histone acetyltransferases is responsible for spermidine mediated longevity.

As the role of the Sir2p deacetylase is well established in replicative ageing^{15, 16}, we tested its potential involvement in polyamine-promoted longevity during chronological ageing. Deletion of *SIR2* did not abrogate the ability of spermidine to extend the chronological life span (data not shown; Table S1). Thus, the observed hypoacetylation during chronological life span extension is not due to the sole induction of Sir2p activity. Similarly, deletion of each of the other known yeast sirtuins (*HST1*, *HST2*, *HST3*, *HST4*) did not affect longevity upon spermidine application (Table S1). This result is compatible with previous findings suggesting that chronological life span extension is not mediated by Sir2p activity¹² nor by any of the other yeast sirtuins¹⁷.

Theoretically, spermidine treatment could lead to hypoacetylation either via activation of histone deacetylases or via inhibition of histone acetyltransferases (HATs). We therefore

investigated whether the disruption of each of the 28 genes involved in histone (de)acetylation would affect chronological ageing in the presence or absence of spermidine. The anti-ageing (pro-survival) effect of spermidine was partially abrogated only upon deletion of genes involved in the process of histone acetylation, e.g. $\Delta iki3$ and $\Delta sas3$ (Table S1). These findings suggest that inhibition of histone acetyltransferases rather than activation of histone deacetylases is responsible for histone H3 hypoacetylation and life span extension upon spermidine application.

Autophagy is required for maximum longevity of chronologically ageing yeast.

Autophagy has been suggested to play an important role in various scenarios of longevity¹⁸⁻²⁰. Accordingly, autophagy-deficient $\Delta atg7$ cells exhibited higher death rates than wild type cells (due to necrosis as well as apoptosis) during yeast chronological ageing (Fig. S6e). Deletion of *ATG7* also compromised the life span extending effects of spermidine application in yeast (Fig. 6d, e), although survival could be protracted by spermidine early during ageing (Fig. 6d). This indicates that autophagy is crucial for maintaining full viability during polyamine-dependent life span extension. Similar results were observed when autophagy was blocked by deletion of *ATG6* or *ATG8* instead of *ATG7* (data not shown). Since $\Delta atg7$ cells could still be rescued early during ageing, autophagy-independent "backup" mechanisms may also be elicited by spermidine.

Supplementary References

1. Balasundaram, D., Tabor, C. W. & Tabor, H. Spermidine or spermine is essential for the aerobic growth of *Saccharomyces cerevisiae*. *Proc Natl Acad Sci U S A* 88, 5872-6 (1991).
2. Chattopadhyay, M. K., Tabor, C. W. & Tabor, H. Polyamine deficiency leads to accumulation of reactive oxygen species in a *spe2Delta* mutant of *Saccharomyces cerevisiae*. *Yeast* 23, 751-61 (2006).
3. Madeo, F. et al. Oxygen stress: a regulator of apoptosis in yeast. *J Cell Biol* 145, 757-67 (1999).
4. Madeo, F., Frohlich, E. & Frohlich, K. U. A yeast mutant showing diagnostic markers of early and late apoptosis. *J Cell Biol* 139, 729-34 (1997).
5. Madeo, F. et al. A caspase-related protease regulates apoptosis in yeast. *Mol Cell* 9, 911-7 (2002).
6. Wissing, S. et al. An AIF orthologue regulates apoptosis in yeast. *J Cell Biol* 166, 969-74 (2004).
7. Buttner, S. et al. Endonuclease G regulates budding yeast life and death. *Mol Cell* 25, 233-46 (2007).
8. Fahrenkrog, B., Sauder, U. & Aebi, U. The *S. cerevisiae* HtrA-like protein Nma11p is a nuclear serine protease that mediates yeast apoptosis. *J Cell Sci* 117, 115-26 (2004).
9. Burtner, C. R., Murakami, C. J., Kennedy, B. K. & Kaerberlein, M. A molecular mechanism of chronological aging in yeast. *Cell Cycle* 8, 1256-70 (2009).
10. Longo, V. D. & Finch, C. E. Evolutionary medicine: from dwarf model systems to healthy centenarians? *Science* 299, 1342-6 (2003).
11. Burhans, W. C. & Weinberger, M. Acetic acid effects on aging in budding yeast: Are they relevant to aging in higher eukaryotes? *Cell Cycle* 8 (2009).
12. Fabrizio, P. et al. Sir2 blocks extreme life-span extension. *Cell* 123, 655-67 (2005).
13. Fabrizio, P. et al. Superoxide is a mediator of an altruistic aging program in *Saccharomyces cerevisiae*. *J Cell Biol* 166, 1055-67 (2004).
14. Weinberger, M. et al. DNA replication stress is a determinant of chronological lifespan in budding yeast. *PLoS ONE* 2, e748 (2007).
15. Longo, V. D. & Kennedy, B. K. Sirtuins in aging and age-related disease. *Cell* 126, 257-68 (2006).
16. Lin, S. J., Defossez, P. A. & Guarente, L. Requirement of NAD and SIR2 for life-span extension by calorie restriction in *Saccharomyces cerevisiae*. *Science* 289, 2126-8 (2000).
17. Smith, D. L., Jr., McClure, J. M., Matecic, M. & Smith, J. S. Calorie restriction extends the chronological lifespan of *Saccharomyces cerevisiae* independently of the Sirtuins. *Aging Cell* 6, 649-62 (2007).
18. Juhasz, G., Erdi, B., Sass, M. & Neufeld, T. P. Atg7-dependent autophagy promotes neuronal health, stress tolerance, and longevity but is dispensable for metamorphosis in *Drosophila*. *Genes Dev* 21, 3061-6 (2007).

19. Tavernarakis, N., Pasparaki, A., Tasdemir, E., Maiuri, M. C. & Kroemer, G. The effects of p53 on whole organism longevity are mediated by autophagy. *Autophagy* 4, 870-3 (2008).
20. Melendez, A. et al. Autophagy genes are essential for dauer development and life-span extension in *C. elegans*. *Science* 301, 1387-91 (2003).